Structural phase stability of $B2$ and $B32$ intermetallic compounds

N. E. Christensen*
Max-Planck-Institut für Festkörperforschung, D-7000 Stuttgart 80, Federal Republic of Germany
(Received 28 January 1985)

For each of the compounds CsAu, LiAu, LiB, LiAl, LiGa, LiIn, LiTl, LiZn, LiCd, LiHg, NaIn, and NaTl the difference is calculated between the total energy of the compounds in the $B2$ (CsCl) and $B32$ (NaTl) crystal structures. The calculations are carried out over a pressure (P) range large enough to predict pressure-induced phase transitions. The structural differences in free energy at $P=0$ agree in sign with the observation of stable structures. The bonding of CsAu and LiAu appear to be quite different: CsAu is ionic and LiAu metallic. In the present theory where only these two structures are compared, CsAu has, at $P=0$, the $B2$ structure, but is predicted to undergo a transition to $B32$ at $P\approx 45$ kbar. LiAu is, according to the calculations, not stable at $P=0$ in the CsCl structure; it requires an external pressure >145 kbar to exist in that structure. Trends of structural energy differences for the I-II and I-III compounds are analyzed by the examination of charge distributions, partial pressures, and their relation to constituent-atom "sizes." The I-II and I-III compounds which at $P=0$ have the NaTl structure are predicted to undergo a structural phase transition at moderately high pressure (~ 200 kbar for LiAl). The bonding characteristics are examined by calculation of (nonspherical) charge distributions. Further analysis is supported by "frozen-potential" energy-difference calculations. The (hypothetical) LiB compound is the only one among the Zintl phases studied here which is semiconducting. It is also the case in which the covalent bonding is most pronounced. A few results of calculations for other compounds with structures related to those of the main topic of the work are also presented. These are for the pnictides, Li_3Sb and Cs_3Sb, which, in spite of expected similarities, show substantial differences as far as charge distributions are concerned.

I. INTRODUCTION

The density-functional formalism[1] and its approximate description in the local-density approach[2–5] has been applied successfully in several theoretical predictions of phase stability and pressure-induced phase transitions in solids.[6–9] One reason for the recent rapid development of this field of theoretical solid-state physics is the advent of efficient and accurate methods of solving the Schrödinger-like one-electron equation, such as the linear-muffin-tin-orbital (LMTO) method,[10] self-consistent, norm-conserving pseudopotentials,[11–13] and linear combination of Gaussian orbitals[13–15] (LCGO). The methods can now be refined to a degree which allows calculations of vibrational frequencies, phonon anomalies, forces, and elastic constants[16–20] in parameter-free approaches. The present work describes calculations of structural energy differences for a series of intermetallic compounds.

Some I-II metal compounds (LiZn, LiCd) and I-III metal compounds (LiAl, LiGa, LiIn, NaIn, NaTl) crystallize in the $B32$ (Zintl[21]) structure. These compounds have attracted some interest in connection with technological applications, in particular, LiAl which appears to be well suited as electrode material of high-energy-density batteries. The compounds listed here are all metallic, but the I-III compounds have very low metallic conductivity. They, at least LiAl, furthermore, have a defect lattice[22–24] with a finite concentration of vacancies even at low temperatures. The nature of the bonding has been subject to several discussions,[24–27] all of which agree criticizing the picture originally proposed by Zintl and Brauer[21] and Hückel.[28] They[21,28] suggested that in the I-III compounds, the alkali metal transfers its valence electron to the other constituent atom, which then acts as Si in forming a diamond lattice by usual sp^3 bonding. The electronic structure of some of these compounds has been examined earlier; LiAl by Ellis *et al.*,[26] Zunger,[27] and Asada *et al.*[24] Furthermore Asada *et al.*[25] calculated the band structure of LiCd and LiZn. In spite of this we find further calculations important, and we shall in the present work essentially discuss the structural phase stability of the compounds, and in some cases predict, by means of the calculations, pressure-indiced structural phase transitions.

The paper is organized as follows. The method of calculation and the approximations used are briefly described in Sec. II. This section also contains information about the relevant crystal structures. Before discussing the I-II and I-III compounds we wish to illustrate that the accuracy of our method of calculation is sufficient. This is partly done in Sec. II, where the bcc–fcc structural energy difference of Pd is calculated—a particularly difficult case. Further examples are discussed in Sec. III, where the P-V relation for GaAs and $B2$–$B32$ structural energy differences for CsAu and LiAu are calculated. The latter turns out to have some interest beyond that of being merely a test case. Section IV contains the calculated band structures for the I-II and I-III compounds together with density of states, charge distributions, etc. The re-

sults of the total-energy calculations, i.e., structural energy differences, equilibrium volumes, and predicted structural phase transitions follow in Sec. V. In the discussion of the nature of bonding, it appears interesting to include the pnictide compounds Li_3Sb and Cs_3Sb. These calculations are described in Sec. VI. The last section (VII) contains a summary and some concluding remarks.

II. CALCULATION

A. Method of calculation

The total energies are calculated within the local-density approximation (LDA). The actual calculations use the exchange-correlation functional of Ceperley and Alder[29] as parametrized by Perdew and Zunger.[30] The band structures are calculated self-consistently in the "scalar relativistic scheme,"[31–33] i.e., spin-orbit coupling is omitted, except for the cases of LiTl and Cs_3Sb. We use the linear-muffin-tin-orbital method,[10] and always include the so-called[10] "combined-correction term" which corrects for the finite number of terms in the angular-momentum expansion (we include here terms with $l \leq 2$), and further it corrects for the nonspherical shapes of the "cells." This extension beyond the "atomic-sphere approximation"[10] (ASA) is necessary for calculation of total energies.[7,8] This also was clear from our calculation of elastic shear constants.[20] The corrections due to this term at particular levels (Γ_1^c, Γ_{15}^v) in the semiconductors in the zinc-blende structures (GaAs) can be quite large[32,33] (~ 1 eV!). In general, however, the effects of the correction on structural energy differences are not correspondingly dramatic. For example, trends and signs of the structural energy differences through the transition-metal series can be well accounted for even by means of the ASA scheme alone. Difficulties appear,[34,35] however, at the upper end of each transition-metal series. For Pd and Au, for example, the ASA functional predicts the bcc structure to be stable.[34] This is illustrated in Fig. 1, where the dashed curves represent the ASA total energies of Pd (fcc and bcc) as functions of the Wigner-Seitz radius S. The bcc energies clearly are below those of the fcc lattice. Further, the values of S for which the energy is minimum, $S_0 \cong 2.83$ a.u., is somewhat too low compared to experiment, $S = 2.873$ a.u. The curves drawn with solid lines in Fig. 1 represent the total energies calculated with inclusion of the combined-correction term. In this case the fcc energy is the lower, and, in addition, the predicted equilibrium volume is now in excellent agreement with experiment (Fig. 1).

The ASA total-energy functional includes only the $l = 0$ contribution to the intercellular Coulomb interaction. This term vanishes in monoatomic solids, and is for compounds given by the Madelung energy. Some improvement over this approximation can be obtained by calculating the intercellular interactions in a muffin-tin model, i.e., assuming that the charge distribution is spherical symmetric inside nonoverlapping muffin-tin spheres and constant in the interstitial region. This muffin-tin correction, suggested by Glötzel and Andersen[36] was employed in several cases by McMahan and Skriver (see, for example, Ref. 8). There are cases where the contributions

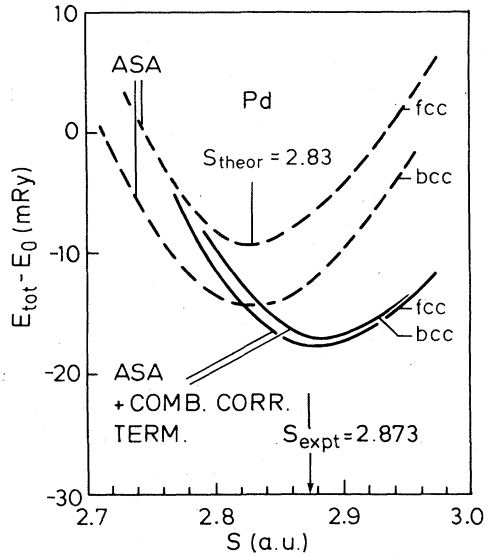

FIG. 1. Total (valence electron) energy (arbitrary reference energy) for bcc and fcc Pd versus Wigner-Seitz sphere radius (S). Dashed curves, self-consistent relativistic ASA; solid curves, self-consistent LMTO with inclusion of the "combined-correction term" (see text and Ref. 10).

from the muffin-tin correction[37,38] term are quite important, and where the ASA functional alone would lead to rather inaccurate results. The calculation of c/a ratios for hexagonal transition metals represents such a case. Figure 2 shows self-consistent calculations of the total en-

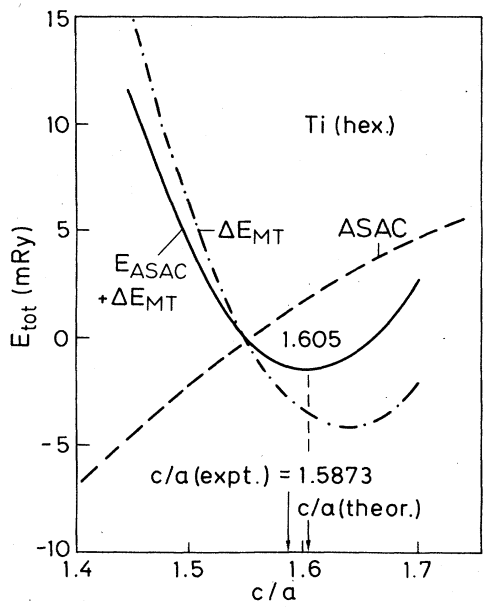

FIG. 2. Calculated variation of the total energy of Ti (hexagonal) with the value of c/a. The dashed curve was calculated within the approximations used to deduce the solid curves in Fig. 1. The dashed-dotted curve is the intercell interaction energy calculated by assuming a charge distribution of the muffin-tin type, i.e., it is assumed that $\rho(\mathbf{r})$ is spherically symmetric inside the (nonoverlapping) muffin-tin spheres and constant in the interstitial region.

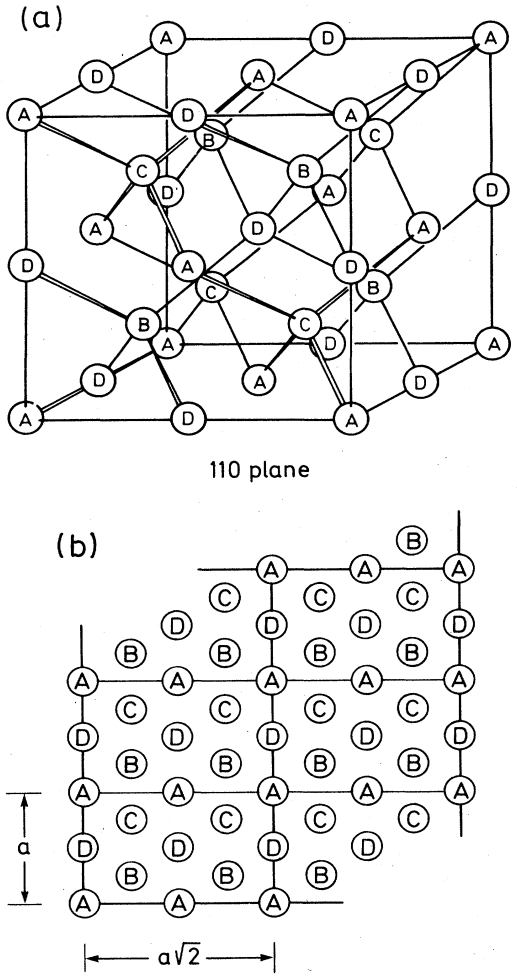

FIG. 3. (a) Face-centered-cubic structure with four basis atoms. The lattice constant is a. (b) (110) plane of the structure in (a) (see Table I).

ergy of Ti (dashed line) versus c/a, and it is seen that no minimum occurs. Only after addition of the "muffin-tin" correction (dashed-dotted line) does the curve (solid line) exhibit a minimum, and the predicted value of c/a is close to the experimentally observed ratio. Similar conclusions were reached by Skriver.[35,37]

The calculations described in the following section include the corrections described here. It is emphasized, however, that the effects on the structural energy differences between the $B2$ and $B32$ structures are much less pronounced than suggested by the examples above. These are extreme cases. Not for a single compound studied in Sec. IV did we find structural differences of the muffin-tin correction big enough to reverse the sign of the difference in free energy at zero pressure, i.e., to affect the conclusions about the most stable structure. If, on the other hand, it had turned out, for the structure determination, to be crucial whether the corrections are included or not, then further refinements should also be examined. In that case we would have had to investigate the change in the total energies due to the actual nonsphericity in the charge distributions.[39,40]

B. Crystal structures

A large number of cubic compound crystal structures can be derived from the structure illustrated by Fig. 3. We consider this to represent a face-centered-cubic structure with basis atoms A, B, C, and D. The lattice constant is a. If all atoms are identical, Fig. 3 represents the bcc structure with lattice constant equal to $a/2$. Letting A and B be equal and C and D vacant, the structure is that of diamond. We give, in Table I, the structure identification for some choices of occupancy of the four sites in the basis. More detailed descriptions and excellent reviews may be found in Refs. 41—45. Table I shows, for example, that LiAs in the CsCl structure ($B2$) would be derived from the $B32$ structure by interchanging the Li and Al atoms on sites C and D. The representations in Fig. 3 and Table I of the diamond and zinc-blende structures simultaneously describe the division of space employed in our actual LMTO calculations for such crystals.[46—52] The LMTO method is particularly accurate for close-packed structures, and therefore "empty spheres" are introduced in the diamond-type lattices (E and $E1$,$E2$ in Table I). These are "atomic spheres" with no nuclear charge, but with finite electronic charge density after completion of the self-consistency iterations. Also, the LMTO calculations of ternary Zintl-phase compounds,[53] examples of which are given in Table I (footnote d), employ empty spheres. Thus, GaAs as well as MgCuSb, in our description, both have four inequivalent "atoms" in the basis.

III. EXAMPLES: GaAs, CsAu, AND LiAu

This section describes briefly calculations of the electronic structures of some compounds in the crystal structures presented in Sec. II B. Details of LMTO calculations for the "test cases" which are chosen may be found elsewhere.[32,33,54—56] The present calculations for CsAu and LiAu, however, differ from those of Refs. 54 and 55 by treating the CsCl structure as the structure described in Sec. II, i.e., the basis contains two formula units, and the Bravais lattice is taken to be fcc. Further, these two compounds are here also studied in the (hypothetical) $B32$ (NaTl) structure, and $B2-B32$ structure energy differences are calculated.

The local-density approximation to the density-functional theory for exchange and correlation leads to s-p valence bands of GaAs that appear to be in excellent agreement with experiments. The conduction bands, on the other hand, lie far too low.[33,56] The gap is only 0.25 eV, i.e., $\frac{1}{6}$ of the experimental value. It was found[33] that the $3d$-core states have to be treated as band states, i.e., they cannot be included in a "frozen" core. The cohesive properties of GaAs are affected by the Ga $3d$ states which contribute somewhat to the bonding. They give at the equilibrium volume a numerically small, negative-pressure contribution, and with these states relaxed, we get an almost perfect agreement with the experimental[57] lattice constant, bulk modulus, and the experimental pressure derivative of the bulk modulus. This is illustrated by Fig. 4, where the calculated P-V relation for GaAs is compared to the experimental[57] data.

TABLE I. Examples of crystal structures derived from Fig. 3 by different choices of occupation of the sites A, B, C, and D.

Structure	Name	Example	Position A (0,0,0)	Position B $(\frac{1}{4},\frac{1}{4},\frac{1}{4})$	Position C $(\frac{3}{4},\frac{3}{4},\frac{3}{4})$	Position D $(\frac{1}{2},\frac{1}{2},\frac{1}{2})$
$A2$	bcc	Cs	Cs	Cs	Cs	Cs
$B2$	CsCl	CsCl	Cs	Cl	Cl	Cs
$B3$	diamond	Si[a]	Si	Si	E	E
	zinc blende (sphalerite)	GaAs[b]	Ga	As	$E1$	$E2$
$B32$	NaTl	NaTl	Na	Tl	Na	Tl
$L2_1$	Heusler alloys	Cu_2MnAl	Cu	Mn	Al	Cu
$D0_3$	BiF_3	β-Li_3Sb[c]	Sb	$Li_{(1)}$	$Li_{(1)}$	$Li_{(2)}$
$B1$	NaCl	NaCl[a]	Na	E	E	Cl
$C1$	CaF_2	Mg_2Sn	Sn	Mg	Mg	E
Cl_3	d	MgLiSb	Sb	Mg	Li	E
	d	MgCuSb	Sb	Cu	E	Mg

[a] E means "vacant."
[b] The two vacancies $E1$ and $E2$ are inequivalent.
[c] Two-Li positions ($Li_{(1)}$) are equivalent.
[d] These compounds are the Zintl phases of the CaF_2- and antifluorite-type structures (Refs. 41—44).

CsAu is—at ambient conditions—a strongly ionic semiconductor, and it is known to crystallize in the CsCl structure. We show, in Fig. 5, the band structure of CsAu calculated in the scalar-relativistic scheme (i.e., spin-orbit coupling is omitted.) The band structure in Fig. 6 is calculated for the $B32$ structure, i.e., with the Cs and Au atoms in positions D and C (Table I) interchanged. CsAu is also, in this structure, a semiconductor. The zero-temperature free energies of the $B2$ and $B32$ phases are shown in Fig. 7 as functions of the (calculated) pressure. Clearly, at $P=0$, the CsCl structure has a lower free energy than the NaTl structure (lower by 7.5 mRy/atom), in agreement with observation that $B2$ is stable. The free energies shown in Fig. 7, suggest that the CsCl structure is not the stable[58] high-pressure phase, at least for P exceeding $P\approx 40$ kbar. This must be taken into account if

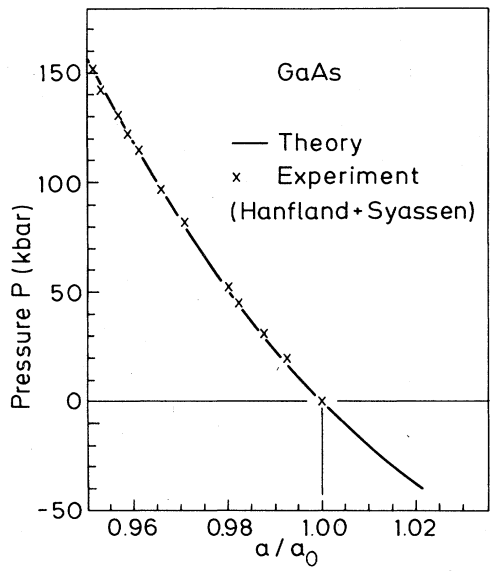

FIG. 4. Pressure (P) versus lattice constant (a) for GaAs calculated (solid line) from self-consistent relativistic LMTO band structures. The "empty spheres" are included (cf. Sec. II), and the Ga $3d$ core states are "relaxed." The crosses indicate experimental results by Hanfland and Syassen (Ref. 57). The equilibrium lattice constant is denoted a_0 ($=5.654$ Å).

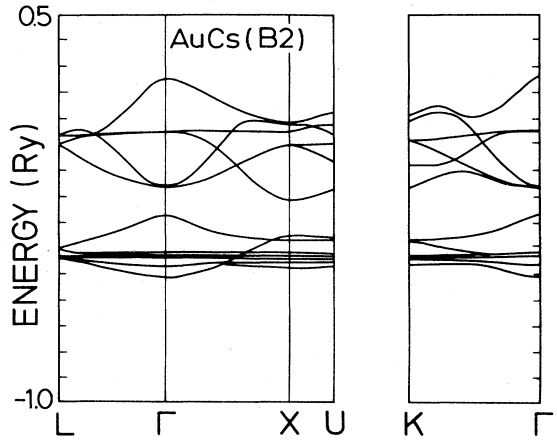

FIG. 5. Band structure of CaAu at the experimental equilibrium volume in the CaCl ($B2$) structure. The bands are shown along symmetry lines in the fcc Brillouin zone as discussed in the text (Sec. II, Table I).

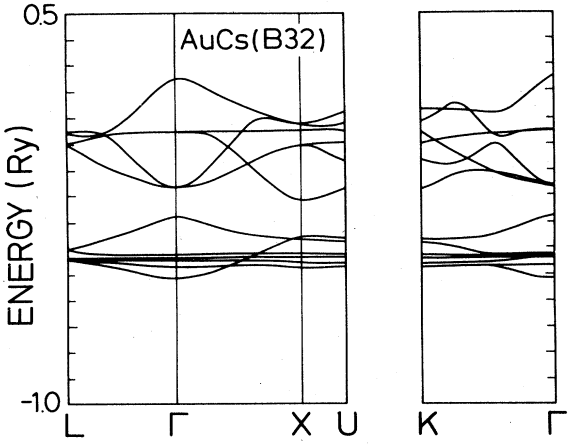

FIG. 6. Self-consistent LMTO (scalar relativistic) band structure of CsAu in the $B32$ structure. The volume is the same as used in the calculation of Fig. 5.

one attempts[54] to predict the pressure at which CsAu becomes metallic.

RbAu is somewhat similar to CsAu in the sense that it is an ionic semiconductor which crystallizes in the $B2$ structure. The stoichiometric compounds of Au with the alkali metals Li, Na, and K, on the other hand, are metals. The crystal structures of these metallic compounds are intricate and not well known—in fact, to our knowledge, the structures of KAu and NaAu are completely unknown. The LiAu compound is often reported to have the CsCl structure which intuitively appears surprising in view of the complexity of the structures of the other two metallic compounds. It is in fact stated[59,60] that LiAu has *not* been observed in the $B2$ structure at stoichiometric composition. Only[59,60] for compounds with 44—45 at. % Au this structure has been established (or maybe more precisely a CsCl-*derived* structure, since some Au atoms are replaced with Li). In view of this we felt it would be interesting to compare the free energy calculated for LiAu in the CsCl structure to the energy in another one, and we have chosen, as this other structure, the $B32$ structure. The total energies as functions of average atomic sphere radius are shown in Fig. 8. It follows clearly from Fig. 8, and from Fig. 9 which shows the Gibbs free energy, that LiAu according to the present theory cannot be stable at $P=0$ in the CsCl structure. The free energy of the $B32$ is much lower, ~47 mRy/(4 atoms) below the $B2$ energy. However, if the $B32$ structure in reality were[60] the stable structure, a transition to the $B2$ structure could be induced by applying a rather moderate pressure, $P_t \approx 145$ kbar (Fig. 9).

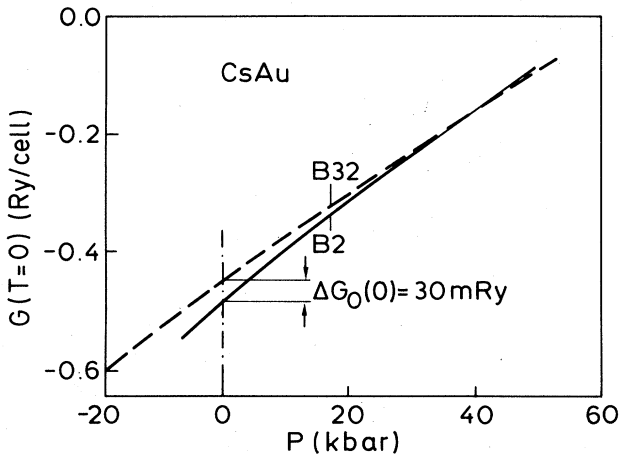

FIG. 7. Pressure dependence of Gibbs free energy ($T=0$ K) (arbitrary reference) for CsAu in the $B2$ and $B32$ crystal structures per two formula units, i.e., per primitive cell in the structure description of Table I.

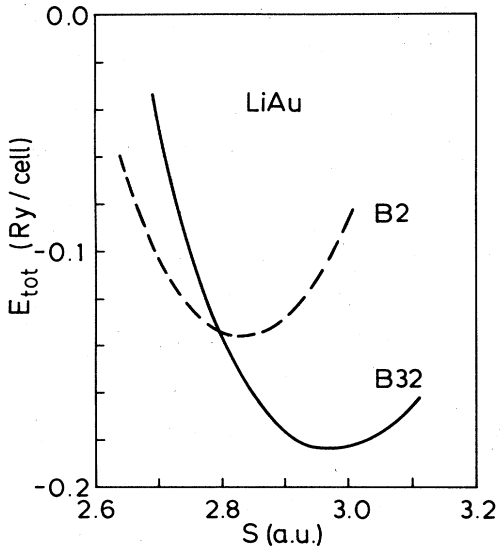

FIG. 8. Calculated total energies for LiAu in (hypothetical) $B2$ and $B32$ structures. [$4(4\pi/3)S^3=a^3/4$, where a is the lattice constant as defined in Fig. 3.]

A common feature of the alkali-metal—gold compounds is the large deviation[54,55] from Vegard's rule. The most ionic compound, CaAu, is most contracted, and LiAu is the compound with equilibrium volume closest to the one which is ideal according to this rule. Still, however, LiAu has a volume contraction of ≈20%. Considering the chemical compositions of LiAu and CsAu one might expect these two compounds to have many properties in common. This is not the case. Rather, they appear to be surprisingly different. The calculations described above already indicate some of these differences—CsAu is

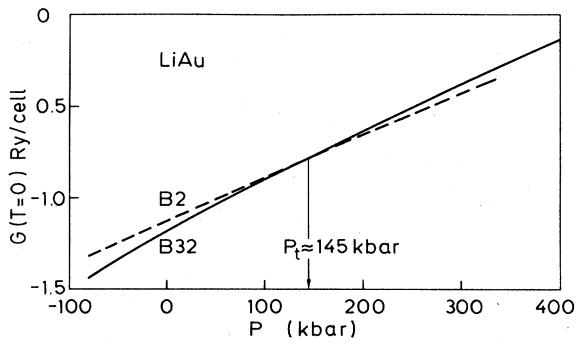

FIG. 9. LiAu. Gibbs free energy for $B2$ and $B32$ structures versus pressure.

a semiconductor whereas LiAu is a metal. CsAu crystallizes in the $B2$ structure and only under pressure can the $B32$ structure be stable. The other compound, LiAu, behaves, expressed somewhat imprecisely,[60] in the opposite fashion. We may explain this in terms of the much smaller size of the ionic core of the Li atom as compared to that of cesium.[61] The compounds NaAu, KAu, RbAu, and CsAu all deviate more from Vegard's law than does LiAu, but nevertheless LiAu is the only compound for which the average atomic-sphere radius S at equilibrium is *smaller*[54] than that of pure gold. As a result, marked differences in state occupancies and partial electronic pressures are found when comparing CsAu and LiAu.

Firstly, the gold $5d$ band is much broader in LiAu, and the partial[62] electronic pressure associated with these states is much larger[63] than in CsAu. This is illustrated in Fig. 10, where we show, for the $B2$ as well as the $B32$ structures, the gold d pressures as functions of the total pressure. At $P=0$, the gold d states give small pressure contributions in both CsAu crystals, whereas they, in LiAu, are almost 10 times as large. It is noted, for LiAu, that the Au d pressure (for $P \geq 0$) is *larger* in the $B32$ structure than in the CsCl structure. Thus, considering only these partial pressures, we would conclude that the Au d states favor the $B2$ structure—in contrast to the total effect, summarized in Figs. 8 and 9. This structure is even more favored by the *Madelung contribution* to the total pressure. Considering an arrangement of point charges of equal magnitude, but opposite signs, in the $B2$ and $B32$ structures, it is obvious from purely geometrical considerations that the $B2$ structure will have the lowest Madelung energy (i.e., largest in *magnitude*). This is indeed also what is found in the actual[62] calculations, as shown in Fig. 11. The Madelung terms are large in magnitude in LiAu, particularly for the $B2$ structure. This is a *second* consequence of the small Li *core* radius that the "charge transfers" are large[64] in this compound. The difference between the Madelung terms shown in Fig. 11 reflects only partly the difference in the geometrical arrangement. In addition, the excess number of electrons[63] in the Li spheres is considerably larger in the $B2$ structure than in the NaTl structure; see Fig. 12. It follows that the smaller Li-core radius leads to two effects, as discussed above, that both tend to favor the $B2$ structure over the $B32$ structure, and the fact that $B2$ does not seem to be stable for LiAu, whereas this is the case for CsAu, appears now much more surprising. The solution to this puzzle follows, however, by examining the occupancy of alkali-metal p states. The free Cs and Li atoms have no valence p states (in the present[61] treatment). The number of Cs p states resulting from hybridization upon alloy formation is small, ~ 0.15 electrons/atom at equilibrium. They give, at equilibrium, and for compressed lattices, a positive partial pressure. The situation is quite different in LiAu, where the large excess charge in the Li sphere

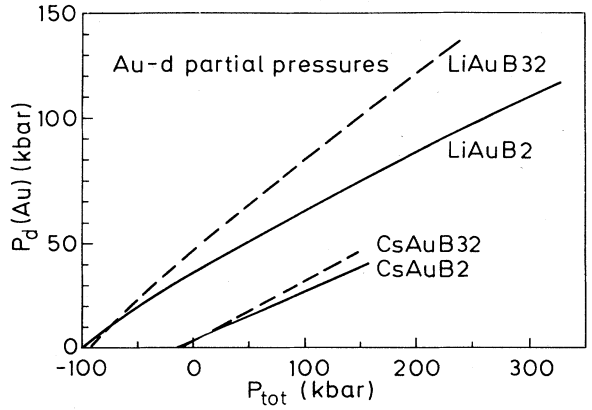

FIG. 10. LiAu and CsAu. The calculated partial pressure from the gold d states as a function of the (calculated) total pressure. The Au d pressures in LiAu are much larger than those in CsAu due to the small ionic core of Li.

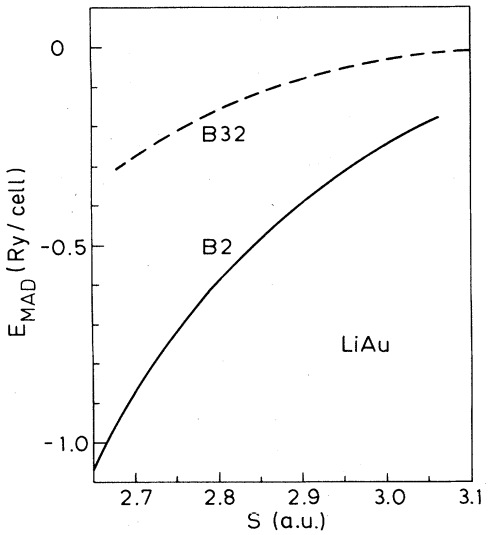

FIG. 11. LiAu. Madelung energy as a function of atomic-sphere radius. In the present LMTO calculation we have chosen the LI and Au spheres to have the same radii, S (see also notes, Refs. 62 and 63).

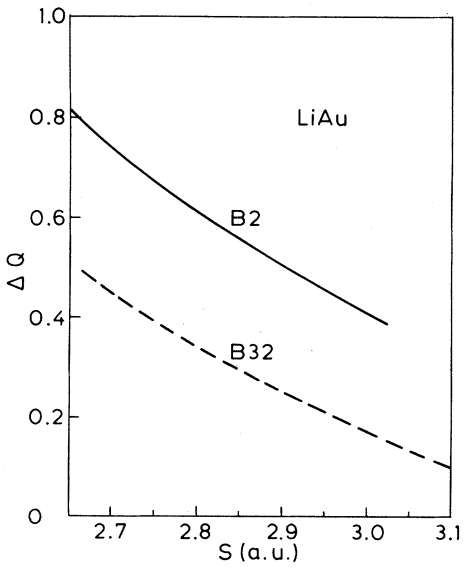

FIG. 12. Excess number of electrons in the LI sphere (see Ref. 64) in LiAu.

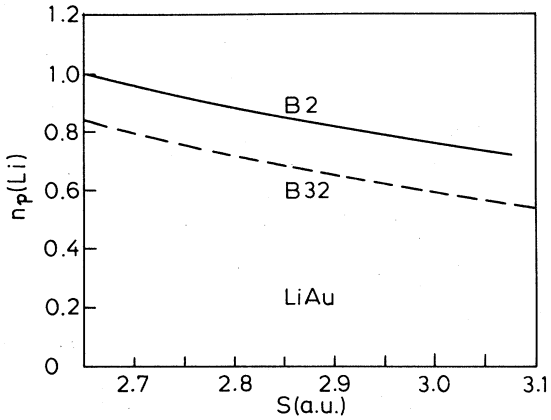

FIG. 13. Number of p electrons in the Li sphere in LiAu versus atomic-sphere radius.

appears as p states; see Fig. 13.

At zero pressure, these p states produce a negative pressure, and although the number of Li p electrons is smaller in the $B32$ structure, they give there a stronger bonding contribution than in the CsCl structure (Fig. 14). Further, the p-state partial pressure remains negative, Fig. 14, over a large range of compression. Thus in LiAu there are two compensating effects resulting from the small Li core: the positive Au d pressure and the bonding (negative) Li p contribution. They determine the equilibrium volume, however, also competed by the Madelung term. The rapid increase in magnitude of this term in the $B2$ structure with compression (Fig. 11) and the simultaneous saturation of the bonding effect from the Li p states (Fig. 14) then drive the transition into the $B2$ structure. The situation for CsAu may be characterized as the opposite: the larger alkali-metal constituent is "compressed" in the alloy, but Au is "expanded." Electrons are transferred from Cs to Au, and the ionic compound is formed. In CsAu there is no large positive Au d pressure to be compensated, and the equilibrium structure is mainly determined by Madelung energy of the ionic charges. Under compression, the ionicity increases more rapidly for the $B32$ structure (not shown here) than for $B2$, and eventually the Madelung term drives CsAu from $B2$ into $B32$ under pressure.[58]

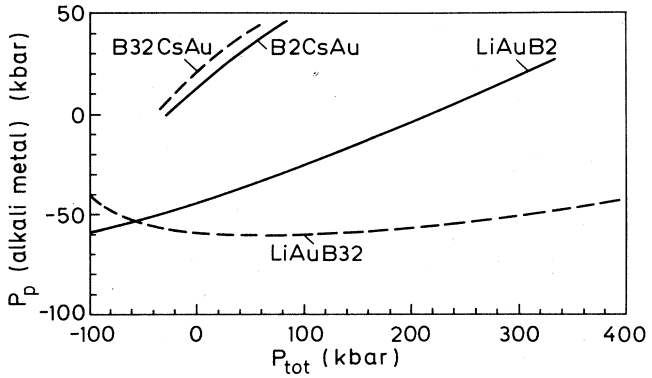

FIG. 14. Alkali-metal p-state partial pressures as functions of the total (calculated) pressure for CsAu and LiAu.

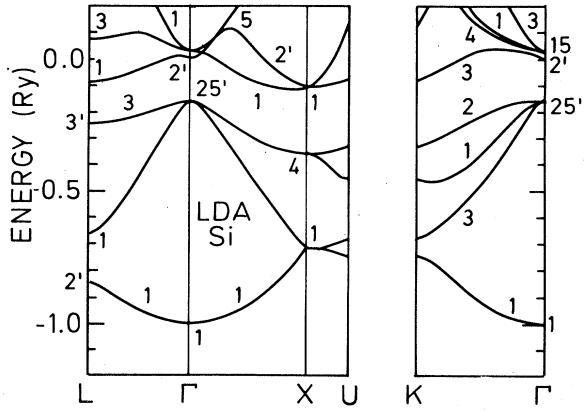

FIG. 15. Band structure of Si calculated by the LMTO method ("empty spheres" are included) and using the local-density approximation. Note the qualitative similarities between this band diagram and that of LiAl (Fig. 16).

There are several reasons why it has been considered worthwhile to include LiAu and CsAu in the present study. First of all, the alkali-metal—gold compounds have interesting physical properties. Although they are considered to form a series with smooth trends, it follows from the discussion here that the compounds at the two opposite ends of this series, in fact, have more remarkable differences than similarities. Further, the behavior of Li in LiAu resembles very much that in the Li compounds discussed in the following, particularly concerning the large number of Li p electrons and the important role which they play in the binding of the crystals.

IV. BAND STRUCTURES OF I-II AND I-III COMPOUNDS

Qualitatively, the band structure of LiAl and the other compounds have similarities with the group-IV semiconductors Si and Ge. This can be seen from Figs. 15 and 16, respectively, which show the energy bands calculated within the local-density approximation for Si and LiAl, the latter in the $B32$ structure. LiAl has a small gap at Γ, and its lowest "conduction band" drops down near X,

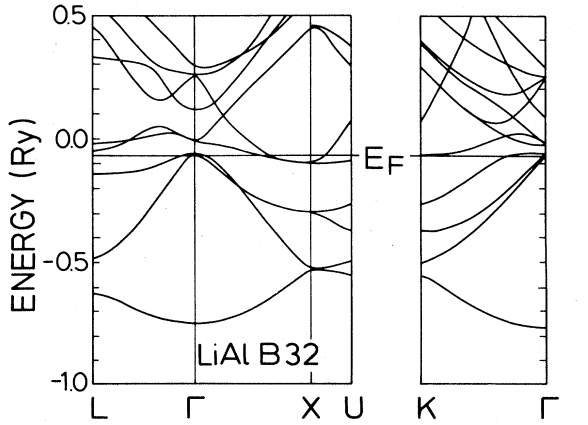

FIG. 16. Band structure calculated for LiAl in the $B32$ structure.

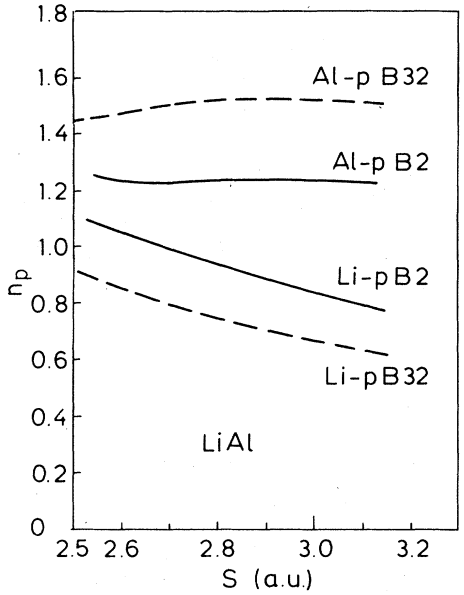

FIG. 17. Number of p electrons in the Li and Al spheres in LiAl as functions of sphere radius S. Results for the $B32$ (dashed lines) as well as $B2$ (solid lines) structures are shown.

very similar to the case of Si. However, in LiAl this band drops so far down that at X it lies below the p-band top Γ_{25} at Γ, and LiAl is a metal (or semimetal). Zunger[27] and Asada *et al.*[24] studied the band structure of LiAl, and their results are quite similar to ours (Fig. 16). From his detailed analysis, Zunger[27] concluded that the bonding in LiAl is a composite of covalent ionic character in the Li—Al bonds and metallic Al—Al bonds, while the Li-Li contacts are essentially nonbonding. References 24 and 27 also agree in the discovery of a large promotion into Li p states just as we also find here, and as was found (Sec. III) for LiAu. Figure 17 shows the volume dependence of the p occupancies for Al and Li in LiAl in the $B2$ and $B32$ structures. For Al as well as Li there are substantially increased numbers of occupied p states over those of the free atoms. It further follows from Fig. 17 that the number of Al p states is larger in the $B32$ structure than in $B2$, whereas the opposite is found for the Li p states. Zunger[27] concluded that no indication of a Li^+Al^- ionic structure could be found. We have calculated the charge distribution in bcc Li, bcc Al, and LiAl all self-consistently at the same atomic volumes (i.e., same S). The difference in radial charge for Al (pure) and Al in the compound, and similar results for Li, show that in LiAl a large part of the charge redistribution takes place in the outer part of the atomic spheres, as is characteristic for metals. [CsAu represented, on the other hand, a typical ionic case (see Refs. 54 and 55), since their electrons were transferred to the *inner* part of the Au sphere.]

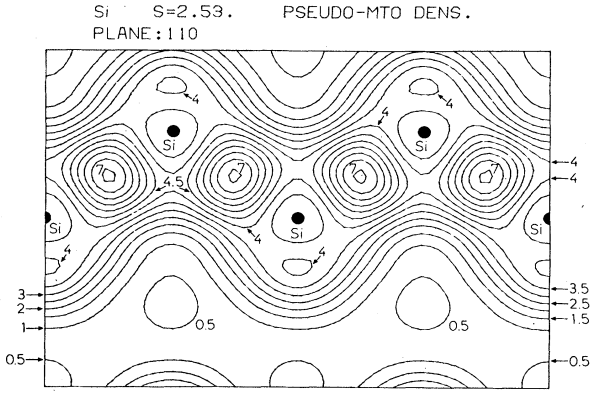

FIG. 19. Similar to Fig. 18, but for Si.

The details of the bonding are, of course, not easy to deduce from the charge densities which have been spherically averaged. We have therefore calculated the nonspherical electron distributions. In Fig. 18 we show the

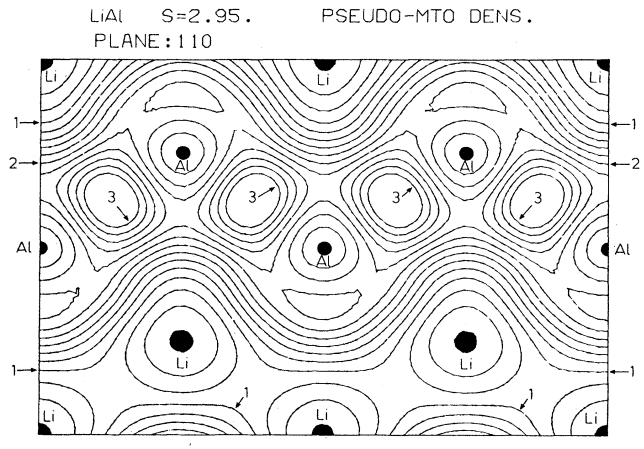

FIG. 18. Electron-density contour plots in the (110) plane of LiAl. Only valence states are considered. The numbers on contours give the density in $10^{-2}\times$[number of electrons/(bohrs)^3]. The density which is plotted is the "pseudo-MTO" density (see Ref. 40). It is very similar to what would be obtained from pseudopotential calculation.

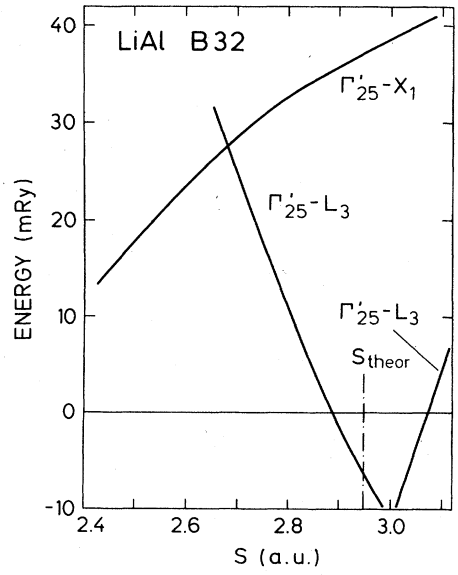

FIG. 20 LiAl. Volume dependence of some Γ-L and Γ-X energy differences.

"pseudo-muffin-orbital" density[40] for LiAl in the $B32$ structure. There is a clear pileup of charge in the Al—Al bonds. It is interesting to compare the density contours of LiAl to those obtained for Si (Fig. 19). The self-consistent band structure (Fig. 15) and the density contours (Fig. 19) of Si were calculated by placing "empty spheres" at positions A and B (Fig. 3) and Si on C and D, i.e., Fig. 19 corresponds to Fig. 18 in the sense that Li has been replaced by an "empty sphere" and Al by silicon. The similarities between the Si contour plot and that of LiAl are striking. Considering the actual values of the densities (Figs. 18 and 19), it follows that the maximum density in the Al—Al bond is considerably lower than that in Si; the ratio is approximately 0.5. This mainly reflects the fact that the volume of Si is smaller than that of LiAl, $V_{\mathrm{Si}}/V_{\mathrm{LiAl}} \sim (2.53/2.95)^3 \sim 0.63$. This difference in volume is, of course, a consequence of the bonding in Si being stronger than that in LiAl, but in spite of this difference in "strength," we conclude that the bonding nature in LiAl is very similar to that in Si. Thus, in the case of LiAl, we arrive at a bonding picture which, at least approximately, is not very far from the model originally suggested by Zintl and Brauer.[21] The finding that there is an (approximate) formation of sp^3 hybrids in LiAl is in accord with the comparison to pseudopotential perturbation theory, which will be discussed in Sec. V B. The fact that we could not, from the charge distributions in the spherical model, find an ionic structure (as mentioned above) does not represent any controversy with the bonding picture outlined here. It simply reflects the fact that the spherical charge-distribution approximation in conjunction with an arbitrary choice of space division (in this case, into equally sized spheres) only allows very crude distribution models.

LiAl is metallic in the $B32$ structure (Fig. 16 and Refs. 24 and 27). Since the X_1 level moves upwards with respect to the Γ'_{25} state under compression, it might be expected that a metal-insulator transition could occur in LiAl when a pressure is applied. This is not the case, as follows from Fig. 20, where the volume dependence of some energy differences is shown. At equilibrium there is an indirect Γ-L gap (and, of course, a *"negative"* Γ-X gap), but the Γ-L gap is quickly closed when the volume is reduced. Neither by compression nor by expansion (in the regime considered here) do we find any isostructural metal-insulator transition. The metallic character is even more pronounced in the band structure when calculated in the CsCl structure, since the X_1 level there drops far below the p-band top at Γ. We have decided to illustrate this by showing the $B2$ and $B32$ band structures, Fig. 21, for another compound in the same family, LiCd. In $B32$ structure [Fig. 21(a)] the gap at Γ is closed, and, in addition (as in LiAl), X_1 lies slightly below Γ'_{25}. LiCd in the $B2$ structure has a gap at Γ, but the gap at L is now closed [Fig. 21(b)], and, as mentioned above, the X_1 level has dropped down. The band structure of LiCd further differs from that of LiAl by the presence of the high-lying Cd d bands. They are (Fig. 21) located just below the Li s—band bottom, and are sufficiently wide to contribute essentially to the bonding. This compound in the $B32$ structure was studied together with LiZn by Asada

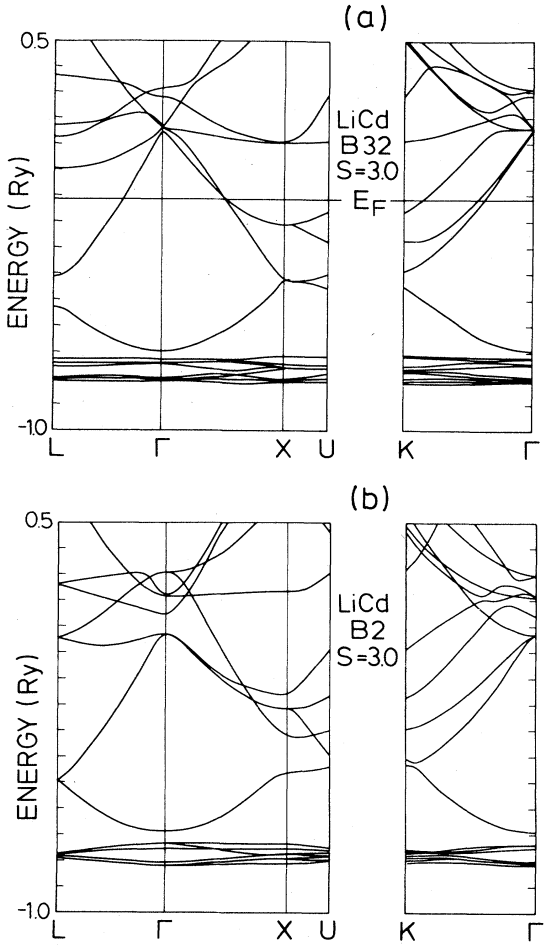

FIG. 21. (a) Band structure of LiCd in the $B32$ structure which is the stable one at zero pressure. (b) LiCd. Band structure calculated for the CsCl structure at zero pressure.

et al.,[25] who described the large number of p states also found here as an intrasite s to p promotion.

Proceeding to LiTl, the closing of the gap becomes more "efficient," as can be seen from Fig. 22, which shows the results of the (scalar-relativistic, as in the previous cases) band calculations for $B2$ as well as $B32$ structures. The Tl s state, Γ'_2, lies far below the Γ'_{25} state (p-like, mainly Tl). The relativistic effects are here large, and they push the Tl s state down (cf. CsAu, Refs. 54 and 55). The Fermi surfaces are entirely different in the two structures. The Tl p states which, in the CsCl structure [Fig. 22(b)] are above E_F, have, in the NaTl structure, moved below E_F, and also the X levels are shifted dramatically. Tl has $Z=81$, and therefore spin-orbit splittings are large. The spin-orbit coupling was included in the band-structure calculation used to produce the density-of-states curves shown in Fig. 23.

LiTl is the only compound among the I-III compounds studied here that clearly, according to the calculations (Sec. V), prefers the CsCl structure to $B32$. Sodium thallide, on the other hand, has the $B32$ structure, which is often also simply referred to as the NaTl structure. A comparison between calculated characteristic parameters

TABLE II. Occupation numbers (n_l), "charge transfer" (ΔQ, see Ref. 64), and Madelung energy (see Refs. 62 and 64) for LiTl and NaTl calculated self-consistently. Results are shown for two volumes ($S=3.00$ and 3.20 a.u.) and two crystal structures ($B2$ and $B32$).

Compound, structure	S (a.u.)	$n_l(M_{\rm I})$ s p d	$n_l(M_{\rm III})$ s p d	$\Delta Q=n(M_{\rm I})-Z_{M{\rm I}}$	$E_{\rm Mad}$ (Ry)
LiTl, $B2$	3.00	0.464	1.380		
		0.916	1.104	0.55	−0.574
		0.274	9.862		
LiTl, $B32$	3.00	0.386	1.350		
		0.744	1.416	0.41	−0.143
		0.214	9.890		
NaTl, $B2$	3.00	0.470	1.440		
		0.688	1.210	0.45	−0.322
		0.332	9.860		
NaTl, $B32$	3.00	0.382	1.268		
		0.534	1.550	0.18	−0.041
		0.274	9.892		
LiTl, $B2$	3.2	0.456	1.490		
		0.796	1.106	0.34	−0.296
		0.234	9.918		
LiTl, $B32$	3.2	0.278	1.468		
		0.644	1.392	0.21	−0.047
		0.186	9.950		
NaTl, $B2$	3.2	0.464	1.535		
		0.712	1.200	0.30	−0.152
		0.272	9.918		
NaTl, $B32$	3.2	0.380	1.484		
		0.476	1.488	0.077	−0.007
		0.222	9.995		

for these two compounds is therefore interesting, and some data obtained from the self-consistent calculations at two different volumes are listed in Table II. A common feature of all eight calculations listed in this table is the large number of p electrons[65] on the sites of both constituents, A and B. The sum $n_p(M_{\rm I})+n_p(M_{\rm III})$ is close to 2 in all cases. For a given compound the $B2$ structure has more $M_{\rm I}$ p states than the $B32$, whereas the opposite occurs for the $M_{\rm III}$ p states. At a given volume, there are more Tl p states in the NaTl compounds than are found in LiTl at the same volume. On the other hand, the Li p occupancies are larger than the Na p values. Table II also gives the excess number[62–64] of electrons in the $M_{\rm I}$ sphere, and the Madelung energy.

V. TOTAL-ENERGY CALCULATIONS FOR I-II AND I-III COMPOUNDS

A. Structural energy differences derived from calculations that are self-consistent for both crystal structures

The total energies and electronic pressures have been calculated (as functions of volume) for LiB (see Fig. 24), LiAl, LiGa, LiIn, LiTl, LiZn, LiCd, LiHg, NaIn, and NaTl, for the $B2$ as well as the $B32$ structure. All the calculations are self-consistent LMTO scalar-relativistic ones, and include the corrections mentioned in Sec. II. We show in Figs. 25–28 the results for four Li compounds, LiAl, LiIn, LiCd, and LiTl. First, it is seen that LiAl and LiTl represent extreme cases in the sense that the former is predicted to favor the $B32$ structure at zero pressure, whereas the CsCl structure is more stable in the case of LiTl. This is in agreement with the observations. Secondly, the structural energy difference between the $B2$ and $B32$ phases as calculated for LiIn and LiCd at ambient pressure are very small—according to the theory they both tend to prefer the sodium thallide structure, but transitions to the $B2$ structure are easy to provoke by applying small pressures. These (marginal) results are quite interesting since experimental observations indicate that LiIn and LiCd crystallize[45] in the $B32$ structure, but they (at least LiCd) are often also found to exist in the CsCl structure. It follows from our total-energy calculations that those compounds that, at zero pressure, have the $B32$ structure all undergo structural phase transitions when

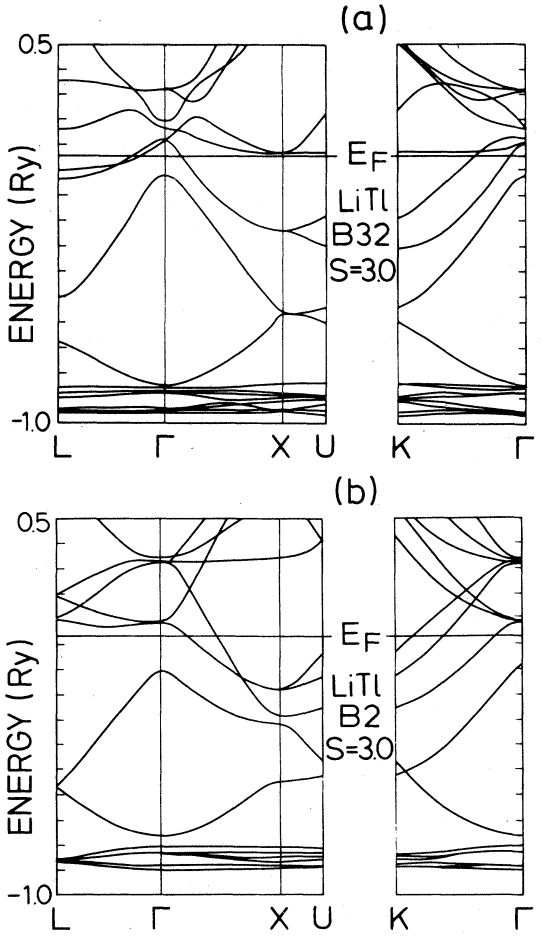

FIG. 22. (a) Band structure of LiTl in the $B32$ structure (spin-orbit coupling omitted). (b) Same as (a) but for the CsCl structure.

pressure is applied—at elevated pressures the CsCl structure becomes more stable than the $B32$ structure. We have not, in the studied pressure regime, seen evidence for a $B2 \rightarrow B32$ transition for LiTl, i.e., we do not expect an instability similar to that predicted for CsAu.

The compounds with sodium, NaIn and NaTl, are both predicted to be much more stable in the $B32$ structure than in that of CsCl.

Figure 29 summarizes the predictions of phase stability of the compounds which we considered here. Shown is the structural difference in free energy (enthalpy) as a function of the atomic number of the group-II or -III constituent. Smooth trends are predicted, when the data are presented in this way. In the "low-Z end" the $B32$ structure is the stable one, but it becomes progressively more unstable with increasing $Z_{M_{II,III}}$. At the "high-Z end" the Li compounds are predicted to prefer the CsCl structure (Fig. 29). From this graph we would also predict, for example, that LiHg has a lower free energy in the $B2$ structure than in $B32$, which is in agreement with experiments and our actual calculation (Table III).

A comparison with experimental data, to the extent that they are available,[66–70] is made in Table III. Here we summarize the signs of the structural free energy as observed, the values calculated, as well as the calculated values of the equilibrium volumes (expressed in terms of the lattice constant a), and the bulk moduli. In addition, we give (Table III) the values, P_t, of the pressure which, according to the calculations, it is necessary to apply in order to provoke a transition from the $B32$ to the $B2$ structure. Apart from the observation[45] mentioned earlier that LiCd at $P \simeq 0$ has been observed in both structures, no experimental results for these transition pressures are, to our knowledge, available.

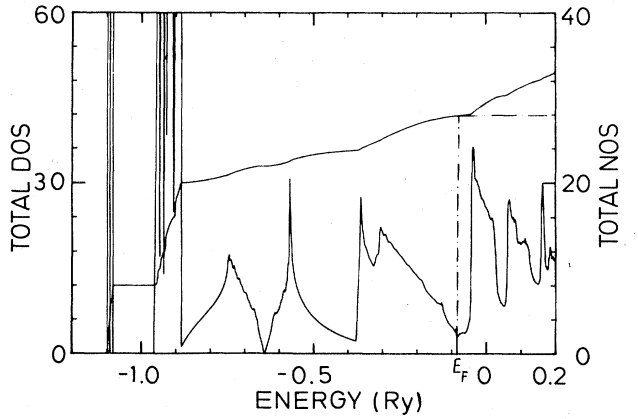

FIG. 23. Density of states (DOS) and number of states (NOS) for LiTl with spin-orbit coupling included. (Partial—density-of states functions may be obtained from the author.)

The calculations which have been performed for the I-II and I-III compounds here agree well with experiments in the sense that equilibrium structures and volumes correspond to the observations. A further analysis is, however, important, and it must answer at least the following questions: (i) Why does LiAl prefer the $B32$ structure and LiTl the $B2$? (ii) Why does the interchange of Li with Na in the Tl compound make the $B32$ structure markedly more stable than the CsCl structure? (iii) Which physical mechanism "drives" the structural phase transition $B32 \rightarrow B2$ under pressure?

Although we do not claim that we were able to carry an

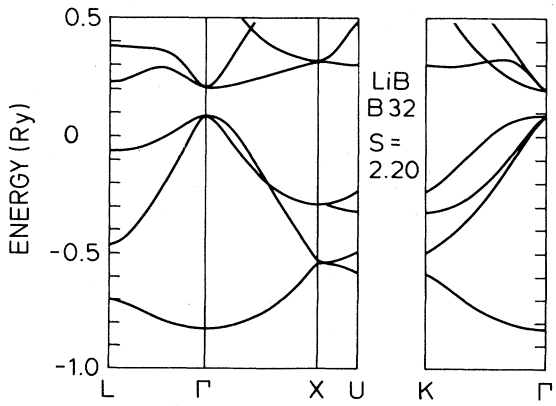

FIG. 24. Band structure calculated for LiB in the (assumed) $B32$ structure. The (average) atomic-sphere radius is $S=2.2$ a.u., corresponding to a volume close to the theoretical equilibrium.

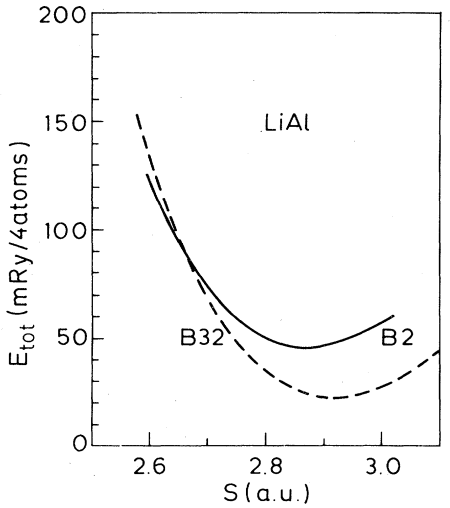

FIG. 25. LiAl. Calculated total energy (arbitrary reference) as a function of atomic-sphere radius S.

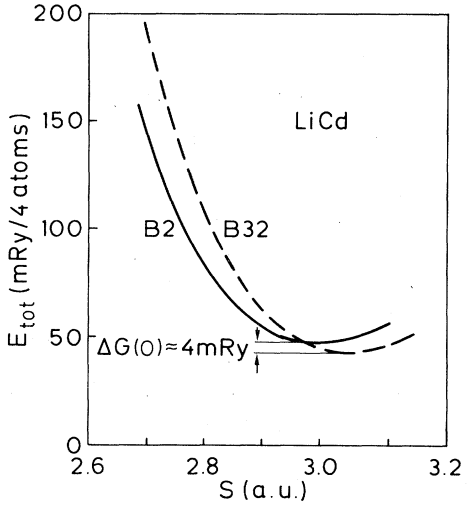

FIG. 27. LiCd. Total energies for the $B2$ and $B32$ structures.

equivalent analysis through in fully satisfactory detail for the alkali-metal—gold compounds (Sec. III), we did gain some insight into the physics determining the stability criteria by discussing the effects of the Li core being much smaller than that of Cs, and by examining partial occupation numbers and partial pressures. A similar attempt will be made here, although some of the quantities are model dependent,[62,64] which complicates the analysis somewhat. In explaining why the $B32$ structure is more stable than $B2$ for LiAu at $P=0$, we argued that the strong hybridization[63] between the Au d states and Li p states—due to the small size of the Li core—on one hand leads to a positive d pressure, which, however, could be compensated for by the bonding of the Li p states. The situation is similar in LiAl, although Al does not possess d states, as does gold. A strong hybridization between Al s and Li p leads to differences between the stability of the two structures. In $B32$ this hybridization implies that the Li p pressure is sufficiently large in magnitude (and negative) when compared to that in $B2$ to make the former structure more stable, at $P=0$. The partial pressures as functions of the calculated total pressure are shown in Figs. 30 and 31, and, further, we give, in Table IV, the partial pressures for both structures at $P=0$. Table IV shows that the bonding due to the Li p—promoted states is, at equilibrium, considerably stronger in the $B32$ structure. On the other hand, the Al p states tend to favor the $B2$ structure, but their negative-pressure contribution is compensated for by the much larger Li s pressure in that structure. In order to examine in more detail the Li and Al s pressures, and the origin of their different magnitudes in the two crystal structures, we may use a decomposition of an *approximate*[38,71–73] pressure expression:

$$(3P\Omega)_l \approx -n_l \left[\frac{\delta C_l}{\delta \ln S} + (\langle E \rangle_l - C_l) \frac{\delta \ln W_l}{\delta \ln S} \right], \qquad (1)$$

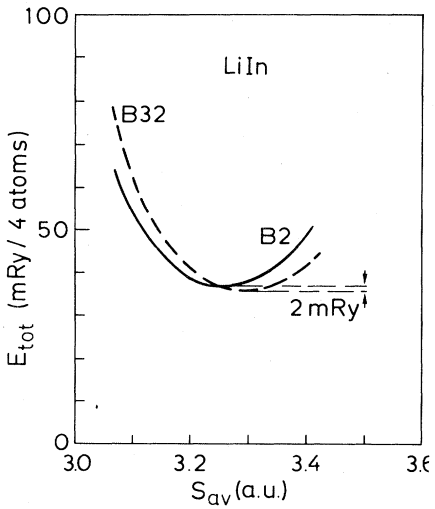

FIG. 26. LiIn. Total energies for $B2$ and $B32$ structures.

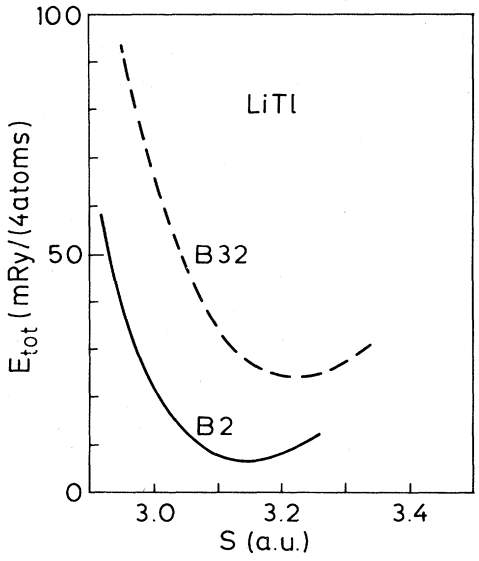

FIG. 28. LiTl. Total energies for the $B2$ and $B32$ structures.

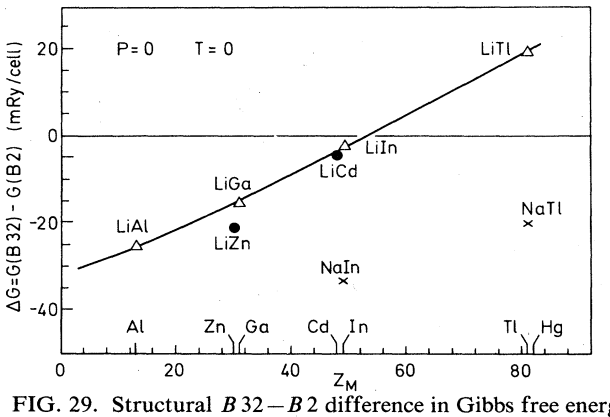

FIG. 29. Structural $B32-B2$ difference in Gibbs free energy for the I-II and I-III compounds considered at $P=0$ and $T=0$, plotted against the atomic numbers $Z_{M_{II}}$ and $Z_{M_{III}}$ of the group-II and -III constituents, respectively.

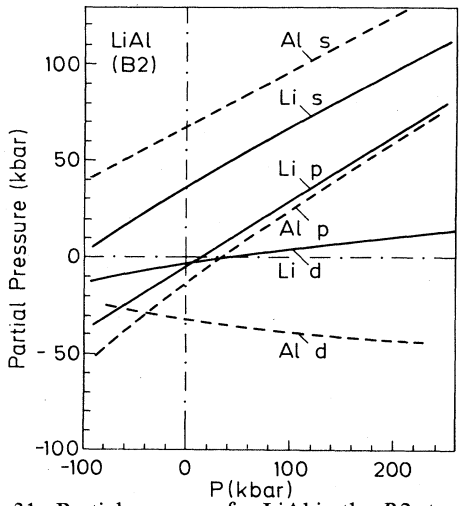

FIG. 31. Partial pressures for LiAl in the $B2$ structure.

where the derivatives are calculated for the "frozen-potential" virtual expansion,[38,71] C_l and $\langle E\rangle_l$ are the band-center parameter and the "center of gravity" of the l band, W_l, is the bandwidth parameter, and n_l is the number of (occupied) states in the l band. For further description of these quantities, we refer to the works on the LMTO method, Refs. 10 and 71–73. The partial pressure, Eq. (1), may be expressed as a sum of three terms, P_{l1}, P_{l2}, and P_{l3}, where

$$3P_{l1}\Omega=\frac{2n_l}{\mu_l}[C_l-V(S)+\mu_{xc}(S)-\epsilon_{xc}(S)]\ , \tag{2}$$

$$3P_{l2}\Omega=n_l(\langle E\rangle_l-C_l)\left[2l+1+\frac{2}{\mu_l}\right]\ , \tag{3}$$

$$3P_{l3}\Omega=-n_l(\langle E\rangle_l-C_l)\frac{2S^2}{D_{\dot{\nu}}+l+1}$$

$$\times[C_l-V(S)+\mu_{xc}(S)-\epsilon_{xc}(S)]\ . \tag{4}$$

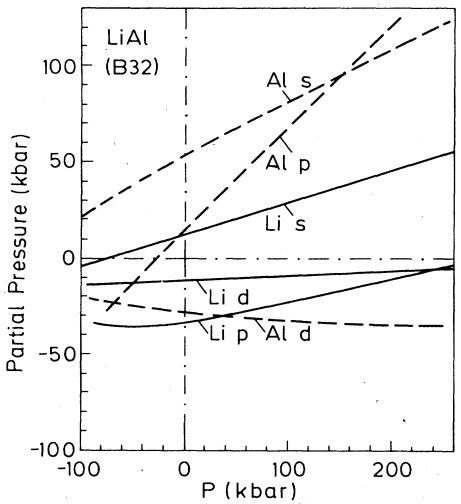

FIG. 30. Partial pressures for LiAl in the $B32$ structure.

Here, μ_l is the mass parameter,[10] and $D_{\dot{\nu}}$ the logarithmic derivative[10] of $\dot{\phi}_{\nu l}$ [the energy derivative of the radial l partial wave evaluated at $E=E_\nu$ (Ref. 10)]. $V(S)$, $\mu_{xc}(S)$, and $\epsilon_{xc}(S)$ are the potential, exchange-correlation potential, and exchange-correlation energy density, all evaluated at the atomic-sphere surface. We give in Table V the values, for the Al s and Li s states at $P=0$, of C, μ, n, $[C-V(S)+\mu-\epsilon]$, and $\langle E\rangle-C$. The values listed in Table V show that the difference between the Li s pressures in the two structures is mainly given by the structural differences in $P_{(\mathrm{Li}\,s)_1}$, i.e., the first term [Eq. (2)] in the approximate pressure relation. The calculation shows that $V+\epsilon-\mu$ in the Li sphere ~ 50 mRy *larger* in the $B32$ structure than in the CsCl structure, and this is due to a larger electron density in the outer part of the Li sphere when calculated (self-consistently) in the $B2$ structure. This charge-density difference reflects the differences in the environment of the Li atoms. In the CsCl structure Li has eight "large" nearest neighbors, Al, whereas it has only half as many nearest neighbors with the longest ranging radial wave functions in $B32$. This is also reflected in the larger "electron transfer" numbers ΔQ (cf. also Table II) found for the $B2$ structure. This picture simultaneously explains why the (outer) Al p states are *fewer* in the $B2$ structure than in $B32$, as also follows quantitatively from Fig. 17. We further understand then that the Al p partial pressure increases more rapidly with compression in the $B32$ structure than in the $B2$. The number of Al p states does *not* increase with pressure (Fig. 17)—rather it decreases. This reflects the strong hybridization to Li states and the fact that it increases rapidly when the volume is reduced. Thus Al p bonding states are "lost," and the Al p pressure increases; this increase with pressure is particularly pronounced in the $B32$ structure (Figs. 30 and 31). For sufficiently large compression of LiAl in the $B32$ structure, the bonding contributions from the Li p and (Al d) states can no longer compensate for the positive Al p pressure, and the $B2$ crystal structure becomes more stable. The phase transition in LiAl at $P\approx 200$ kbar is associated with a volume reduction of $\sim 4\%$. This is

TABLE III. Calculated $B32-B2$ differences ΔG in free energy at $P=0$ and $T=0$, and the stable structure observed. The calculated equilibrium lattice constants a_{theor} and the values measured a_{expt}, as well as the calculated bulk moduli (at theoretical as well as observed equilibrium), are also listed. The pressures P_t are theoretical predictions for $B32\rightarrow B2$ phase transitions. Calculated and measured enthalpy of formation (ΔH) and the temperature used in the experiments are given in the last three columns. (orh. denotes orthorhombic.)

Compound	$G(B32)$-$G(B2)$ [mRy/(formula unit)]	Observed structure	a_{expt} (Å)	a_{theor} (Å)	$B^{t,a}_{\text{theor}}$ (kbar)	$B^{e,b}_{\text{theor}}$ (kbar)	P_t (kbar)	ΔH_{theor}[c] (kcal/mol)	ΔH_{expt} (kcal/mol)	T (expt) (K)
LiB	−96.8			4.797	1690		>10000	−35.8		
LiAl	−12.6	$B32$	6.360	6.328	450	415	200	−11.9 −9.7[d]	−11.6[e] −3.9[e] −5.5[f]	298 900
LiGa	−8.6	$B32$	6.195	6.405[g]	433	709	142	−13.5		
LiIn	−1.3	$B32$	6.786	7.093[h]	347	710	21	−4.4	−11.7[i]	800
LiTl	8.6	$B2$	6.850	6.883	357	385	−85		−9.5[i]	800
LiZn	−12.8	$B32$	6.209	6.027	578	385	550	−11.6	−5.8[f]	820
LiCd	−2.9	$B32$	6.687	6.617	485	430	53			
LiHg	6.3	$B2$	6.580	6.624	443	491	−75		−20[r]	298
NaIn	−14.2	$B32$	7.321	7.518	311	590	>500	−1.3	−4[s]	773
NaTl	−8.8	$B32$	7.488	7.439	299	248	285		−7.8[t]	298
CsAu	15.0	$B2$	8.529	8.297[j]	160[j]	250[j]	40[k]	−1.2		
LiAu	−24.2	orh.	(6.197)	6.040[l]	800[l]	500[l]	145	−16.8[l]		
Cs_3Sb		$D0_3$	9.128	9.415[m]	151	235		−54.0[o] −74.3[p]	−96.5[n]	800
Li_3Sb		$D0_3$	6.572	6.631	343	390		−72.4	−10.8[q]	

[a]Calculated at the theoretical equilibrium volume.
[b]Calculated with $a=a_{\text{expt}}$.
[c]Unless differently indicated, both pure-element structures are taken to be bcc.
[d]Including the theoretical bcc−fcc structural energy difference of 7.2 mRy/atom for Al.
[e]Reference 67.
[f]Reference 68, liquid phase.
[g]Ga $3d$ treated as "frozen-core" states (causes overestimate of a_{theor}).
[h]In $4d$ treated as "frozen-core" states (causes overestimate of a_{theor}).
[i]Reference 69.
[j]See Refs. 54 and 55.
[k]From $B2$ to $B32$.
[l]Calculated for (hypothetical) $B2$ structure.
[m]Cs $5s$ and $5p$ states included in "frozen-core" (causes overestimate of a_{theor}).
[n]Reference 70.
[o]Cs $5s$ and $5p$ states in frozen core.
[p]Two-panel calculation. Cs $5p$ states treated as band states; Cs $5s$ as frozen-core states.
[q]Reference 66.
[r]G. Y. Zukowsky, Z. Anorg. Chem. **71**, 403 (1911).
[s]Liquid phase, T. Kleinsthuber, thesis, Universität München, 1961.
[t]A. Schneider and O. Hilmer, Z. Anorg. Chem. **28b**, 97 (1956).

much smaller than the volume-collapse effect in LiAu (~15%) for the (hypothetical) $B32\rightarrow B2$ transition.[60]

The discussion above for LiAl which identified the "driving mechanism" for the $B32\rightarrow B2$ transition as being intimately related to the overlap between the long-ranging Al p states and the Li states also makes it easy to understand the *trend* of the structural energy differences for the Li compounds. With increasing $Z_{M_{\text{II}}}$ or $Z_{M_{\text{III}}}$, we found (Fig. 29) that the $B32$ structure becomes increasingly unstable—LiIn represents a marginal case—and LiTl is at ambient conditions in the CsCl structure. This we consider a "size effect." The outer p states in Al, Ga, In, and Tl are, in the listed sequence (according to Z), increasingly long ranged, i.e., the compounds in the upper end resemble compressed LiAl in the sense of the description of the partial pressures. Tl in LiTl is so "compressed" that the phase transition has occurred.

The analysis of the charge distributions and partial

TABLE IV. Partial pressures (kbar) for LiAl in the $B2$ and $B32$ structures calculated at volumes at which the (theoretical) total pressure is zero. The value called P_{Mad} is the Madelung contribution (see also Refs. 62 and 64).

	$B2$		$B32$	
	Li	Al	Li	Al
l	s	s	s	s
	p	p	p	p
	d	d	d	d
P_l	35.0	68.0	12.7	53.5
	−4.5	−14.0	−33.5	15.0
	−4.0	−31.7	−11.5	−28.4
$\sum_l P_l$	26.5	22.3	−32.3	40.1
P_{Mad}	−48.8		−7.8	

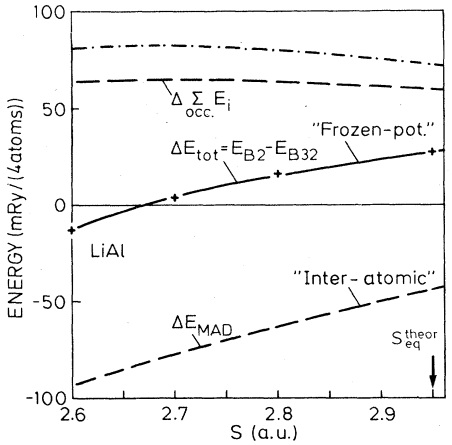

FIG. 32. Frozen-potential calculations for LiAl. The solid line denotes the $B2-B32$ structural energy difference calculated from Eq. (5). The lowest-lying dashed curve gives the Madelung-energy difference [last term in Eq. (5)], whereas the upper dashed curve represents the change in the one-electron energy sum [first term in Eq. (5)]. The dashed-dotted line shows the sum of the band-structure term and the intra-atomic contribution, i.e., it is the difference in one-electron-energy sum plus the $\Delta\rho$ and Δq terms in the large square brackets of Eq. (5). The pluses indicate, for comparison, the energy differences obtained by subtracting the full total energies derived from calculations which are self-consistent in both structures.

pressures showed, for the Li-M_{II} and Li-M_{III} compounds, that a certain difference in "size" of the two constituent atoms is needed in order to stabilize the $B32$ structure at zero pressure, but also that increasing the size[74] of the M_{II} (M_{III}) constituent beyond that of Al acts to destabilize $B32$. It becomes increasingly easy to induce, by applying a pressure, a transition to $B2$. We would now expect it to be in accord with this picture, that replacing—in the Tl compound—Li by Na would restore, approximately, the "ideal" size ratio as found in LiAl for formation of the $B32$ structure. Indeed, NaTl has this structure at ambient conditions, and the structural difference in free energy (Fig. 29) is similar to that of LiAl. Thus the results displayed in Fig. 29 are explained in simple terms. The trends in the I-II series are similar to those of the I-III compounds. Among the Li-M_{II} compounds, LiHg is the only one predicted to have the $B2$ structure, in agreement with observations.

B. "Frozen-potential" method

The total-energy calculations in the preceding subsection demonstrated that the fully-self-consistent calculations give structural $B2-B32$ differences that agree in sign with experiments for the I-II and I-III compounds examined. We have further, in terms of such calculations, tried to investigate the physical mechanism driving the pressure-induced phase transition. It is, however, apparent from that discussion that a very clear model is not easy to present in this way, partly because several of the quantities entering the discussion are strongly dependent on the way in which we decide to divide space.

A very useful supplement to the analysis in Sec. V A can be obtained by a convenient separation of the structural energy difference into contributions which are easily described. Such a separation is obtained by means of a "frozen-potential" approach.[75] This is reminiscent of the "force theorem,"[71,20] which, however, is valid only for infinitesimal distortions. It therefore does not apply to calculations of structural energy differences. We show, in Ref. 75, that the difference in total energy at fixed volume for a compound in two crystal structures, I and II, can be calculated as

TABLE V. Li s and Al s parameters entering the approximate pressure formula, Eqs. (1)—(4), derived from the self-consistent LMTO calculations for LiAl in the $B32$ and $B2$ structures at equilibrium ($P=0$ in both cases).

Constituent	$C_s - V + \mu - \epsilon$ (Ry)	$\langle E \rangle_s - C_s$ (Ry)	C_s (Ry)	μ_s	n_s (states/atom)
		$B2$			
Li	0.440	−0.340	−0.084	0.751	0.443
Al	−0.078	0.120	−0.601	0.969	1.071
		$B32$			
Li	0.390	−0.341	−0.078	0.764	0.440
Al	−0.059	0.100	−0.624	0.969	1.070

$$\Delta F \equiv F(\mathrm{II}) - F(\mathrm{I})$$
$$= \Delta\left[\int_{-\infty}^{E_F} EN(E)dE\right] + \left[\sum_{\mathbf{R}} \int_R \int_R \Delta\rho_R(r)u(\mathbf{r}-\mathbf{r}')\Delta\rho_R(r')d\mathbf{r}\,d\mathbf{r}' + \sum_{\mathbf{R},\mathbf{R}'}{}' \frac{\Delta q_R\,\Delta q_{R'}}{|\mathbf{R}-\mathbf{R}'|_{\mathrm{I}}}\right]$$
$$+ \sum_{\mathbf{R}',\mathbf{R}}{}' q_{\mathrm{II}R} q_{\mathrm{II}R'}\left[\frac{1}{|\mathbf{R}-\mathbf{R}'|_{\mathrm{II}}} - \frac{1}{|\mathbf{R}-\mathbf{R}'|_{\mathrm{I}}}\right]. \tag{5}$$

The band structure is calculated self-consistently for, say, structure I. The effective potentials in the spheres—we use the ASA approximation—are then moved without change (i.e., "frozen") to the positions in structure II. With this arrangement, a single band-structure calculation is then performed. The charges obtained in the spheres, R, from this calculation are called $q_{\mathrm{II}R}$, and the quantities Δq_R and $\Delta\rho_R(r)$ are the changes in charge and density in the spheres. The first term in Eq. (5) is the change in one-electron energy sum and the second (in the large square brackets) is an intra-atomic term, whereas the last is the structural difference in Madelung energy for fixed charges. The potential $u(\mathbf{r}-\mathbf{r}')$ is defined in Ref. 75.

The structural $B2-B32$ energy difference calculated by this frozen-potential method for LiAl is shown in Fig. 32 as a function of (average) atomic-sphere ratio (solid line). The results are very close to those obtained from fully-self-consistent calculations (indicated by pluses in Fig. 32). The band-structure term and the intra-atomic term are essentially volume independent. In a semiquantitative discussion we can omit the intra-atomic term, and we then see from Fig. 32 that the total structural energy difference essentially has been decomposed into two terms of opposite sign: the band-structure contribution and the Madelung term. The band-structure term favors the $B32$ structure, whereas the structural difference in the Madelung energy tends to stabilize $B2$. In an AB compound in $B2$ an A atom has eight B atoms as nearest neighbors, whereas an atom in $B32$ has four like and four unlike atoms in the nearest-neighbor shell. The Madelung energy of a $B2$ lattice is therefore lower than that of a $B32$ crystal of the same volume and charges. This favoring of $B2$ will increase under compression—as also follows from Fig. 32—and eventually the structural Madelung energy difference reaches such a magnitude that the $B32$ structure becomes unstable. The band-structure term, i.e., the difference in one-electron-energy sum might also be referred to as the *covalent* part, since it contains all the effects of bonding and hybridization. When comparing the $B2$ and $B32$ structures of all the I-III compounds included in our study, we find that this term always tends to stabilize $B32$—also in the case of LiTl. The $B32$ structure allows the formations of—more or less complete—sp^3 hybrids, which is an energetically favorable situation.

Although the I-III compounds are not semiconducting, i.e., they do not have a full Jones zone, pseudopotential perturbation theory has been applied with some success. Inglesfield[77] studied the structural stability of NaTl in this way, and his perturbation calculations were later extended by McNeil *et al.*[78] to include essentially all the I-III and I-II compounds, The authors of Ref. 78 partly rejected the interpretation in terms of the "band-structure stabilization" of $B32$ because they (i) found that all compounds in this way were predicted to have the $B32$ structure, i.e., also those which are known to exist in the CsCl structure, and (ii) no clear trends could be found. Admit-

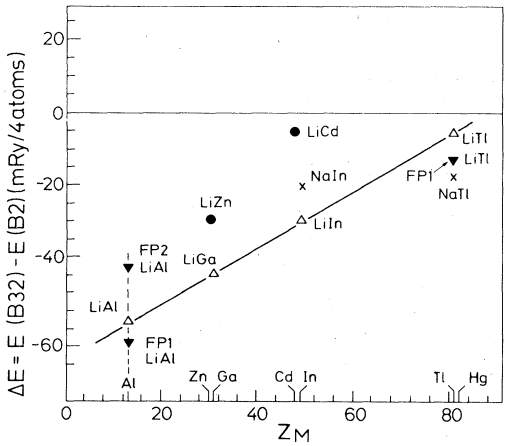

FIG. 33. $B32$-stabilization energies as derived from pseudopotential perturbation calculations by McNeil *et al.* (Ref. 78) plotted against Z_M (as in Fig. 29). These quantities should, in principle, be compared to our "band-structure term" in the frozen-potential (FP) approach (Sec. V B and Ref. 75). This approximate equivalence is illustrated by the solid inverted triangles (FP), which represent the structural difference in one-particle-energy sum alone from the frozen-potential calculations for LiAl and LiTl. The labels FP1 indicate results obtained when the self-consistent calculation is carried out for $B32$, whereas the calculation FP2 corresponds to the case where the $B2$ band structure is self-consistent.

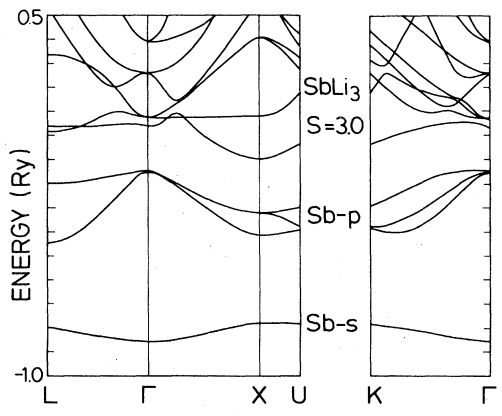

FIG. 34. Band structure of β-Li_3Sb ($S_{av}=3.00$ a.u., i.e., close to equilibrium volume). The valence states consist of low-lying Sb states (around -0.8 Ry) forming a very narrow band, and the Sb states, having their maximum at Γ at ~ -0.1 Ry.

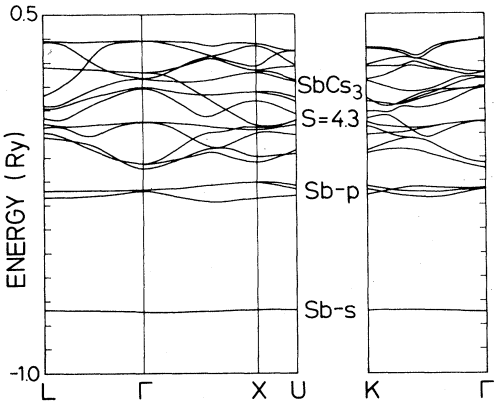

FIG. 35. Self-consistent band structure for Cs_3Sb. The Cs $5s$ and Cs $5p$ states were treated as "frozen" renormalized core states.

tedly, there are large uncertainties in the pseudopotential perturbation calculations; it is necessary[77] to go beyond second order. The procedure is particularly crude for the I-II compounds, which have too few electrons to fill even approximately the Jones zone. If, nevertheless, we present the results of Ref. 78 in a diagram similar to that of our self-consistent energy differences in Fig. 29, we find quite similar trends, as can be seen in Fig. 33. In view of the preceding discussion of the frozen-potential approach, it is not surprising that the $B32$ structure is always favored. The calculated energy differences of Ref. 78 shown in Fig. 33 correspond essentially to our *band-structure term* only, i.e., in our picture it should be compared to the *first term*

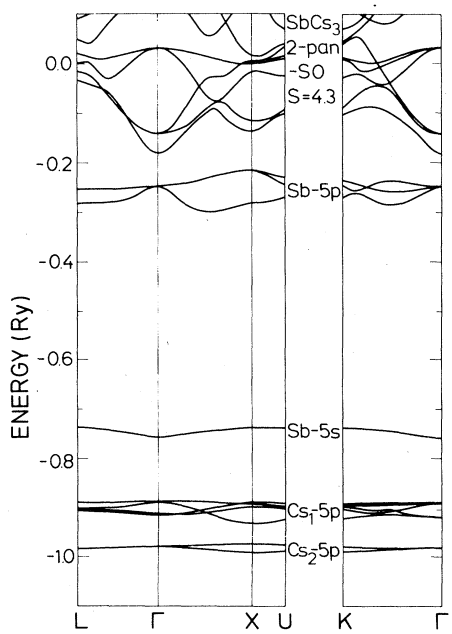

FIG. 36. Scalar-relativistic band structure of Cs_3Sb. The Sb $5s$, Cs $5s$, (not shown), and Cs $5p$ states here are treated as band states, i.e., on the same footing as the upper states during the self-consistency iterations. The calculation was carried out using two energy "panels."

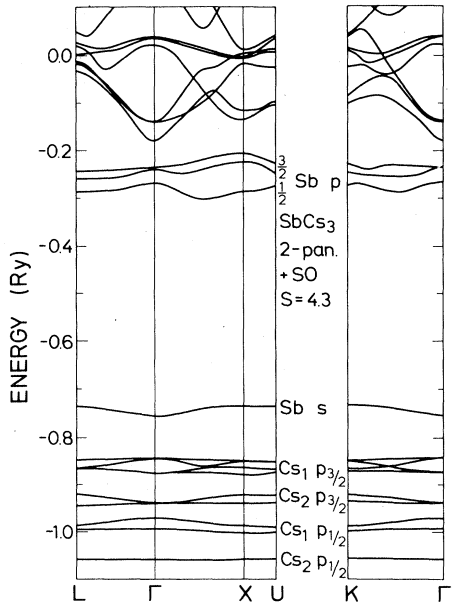

FIG. 37. Dirac-relativistic calculation for Cs_3Sb, i.e., essentially as in Fig. 36, but with inclusion of spin-orbit coupling.

only in Eq. (5). With this modification we then conclude, with the reservations taken about accuracy above, that the physical picture of stabilization of $B32$ from the perturbation calculations by Inglesfield[77] agrees with our analysis. The pseudopotential approach was discussed later by Krasko and Makhnovetskii,[79] and a related examination is presently being carried out by Hafner.[80]

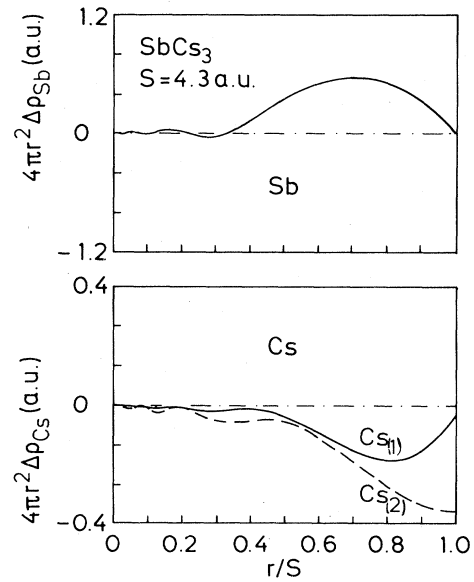

FIG. 38. Change in radial electron densities, $4\pi r^2 \Delta\rho(r)$, due to alloy formation of Cs_3Sb. Upper part: antimony. The integral of the function up to S gives one electron (cf. Table VI). Lower part: density change for Cs. There are two Cs sites of type "1" (B and C in Table I) and one of type "2."

TABLE VI. Li_3Sb and Cs_3Sb: Partial occupation numbers (n_l) and excess number of electrons in constituent atomic spheres (ΔQ). The individual spheres are chosen to have equal radii ($S=S_{av}$). The values of S (4.30 and 3.00 a.u., respectively) are close to the equilibrium values.

Compound A,B,C,D (cf. Fig. 3)	S (a.u.)	$n_l(A)$ s p d	$n_l(B)=n_l(C)$ s p d	$n_l(D)$ s p d	ΔQ A B C D
$SbCs_{(1)}Cs_{(1)}Cs_{(2)}$	4.30	1.912	0.230	0.134	1.066
($SbCs_3$)		4.143	0.178	0.100	−0.270
		0.012	0.322	0.238	−0.270
					−0.524
$SbLi_{(1)}Li_{(1)}Li_{(2)}$	3.00	1.554	0.420	0.310	−0.690
($SbLi_3$)		2.718	0.772	0.510	0.376
		0.038	0.184	0.060	0.376
					−0.060

VI. Li_3Sb AND Cs_3Sb

The antimony-lithium and antimony-cesium compounds which are discussed in this section might, *a priori,* be expected to have many similarities. The outer electronic configurations in the isolated atoms are the same in the two cases, and, indeed, assuming the same crystal structure, the band structures[81] turn out to be similar. Nevertheless, there are, due to the large differences in size of the alkali-metal constituent atom, remarkable differences in the bonding in the two cases. This is also apparent from the different crystal structures observed (see Ref. 43 and references therein). Li_3Sb can exist in hexagonal (α-Li_3Sb) as well as cubic forms (β-Li_3Sb). The cubic structure is isotypic with the BiF_3 structure (Table I), the $D0_3$ structure. At room temperature, Cs_3Sb most probably crystallizes in a NaTl-derived structure with partial disorder, but below $T\sim260$ K it is suggested[82] that it has the ordered $D0_3$ structure. Therefore we have chosen here to study the electronic structures of Li_3Sb and Cs_3Sb in the same (ordered) cubic structure, $D0_3$, i.e., the structure which relates naturally to those of the other compounds discussed in the present article (Table I).

As mentioned earlier, the band structures of Cs_3Sb (when the Cs $5p$ states are treated as core states, i.e., not included as band states) and Li_3Sb are similar. This is seen from Figs. 34 and 35. Both compounds are semiconducting. The band gaps derived from our calculation are, of course, too small when compared to experiments, due to the fact that we use the local-density approximation. For Li_3Sb we find an *indirect* gap which is very small, ~0.14 eV. Cs_3Sb (ordered phase) is also an indirect-gap semiconductor (with $E_g=1.04$ eV), but the nature of the gap is different from that of Li_3Sb (see Figs. 34 and 35). Experiments[83–85] carried out at room temperature, where

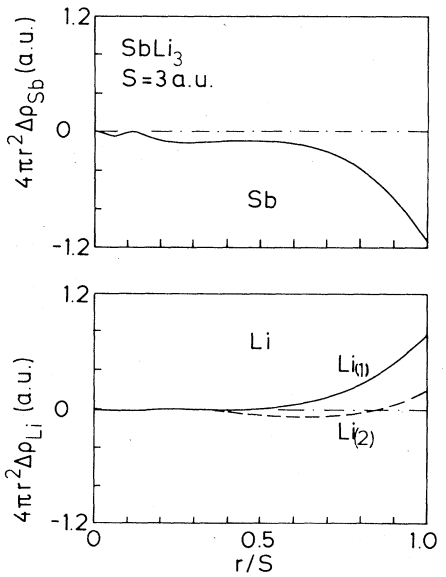

FIG. 39. Same as Fig. 38, but for β-Li_3Sb.

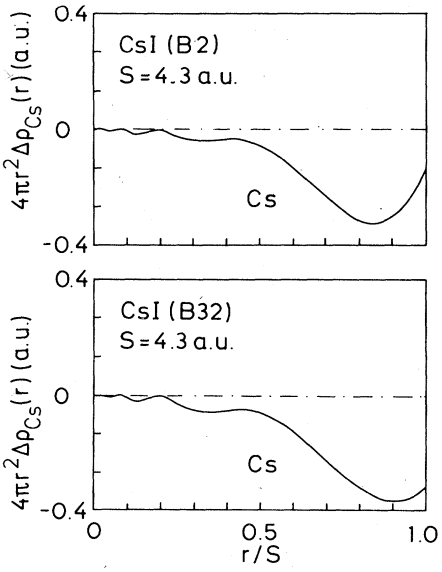

FIG. 40. Radial charge redistribution around Cs due to formation of the CsI compound. (a) refers to the CsCl ($B2$) structure, whereas the results of (b) are for the $B32$ structure. The volumes in both cases are chosen to correspond to $S_{av}=4.30$ a.u., i.e., the same as in Cs_3Sb (Fig. 38).

the disordered phase of Cs_3Sb probably prevails, show that the band gap is $\simeq 1.6$ eV.

The calculated equilibrium lattice constants agree well with experiments. For Li_3Sb we find from total-energy calculations that the average atomic-sphere radius corresponding to equilibrium is $S_{eq}^{theor}=3.035$ a.u. The observed volume[86] corresponds to $S_{eq}=3.057$ a.u. For Cs_3Sb we find $S_{eq}^{theor}=4.30$ a.u. The experimental value quoted by Wyckoff[86] is 4.246 a.u. One reason why the present calculated equilibrium volume is somewhat too large for Cs_3Sb is that the calculation treats the Cs $5p$ states as "frozen," renormalized core states. Including them instead, as band states in the self-consistent calculation leads to a smaller value[54-55] of the theoretical equilibrium volume. The effects in the self-consistent band structure of letting these corelike states relax follow from Fig. 36. Indeed, the Cs $5p$ bands have a appreciable width, which must influence the binding of the crystal. It further follows (Fig. 37) that the spin-orbit splittings of these bands are large, and that this must be taken into account in analyses of optical (photoemission) data.

As stressed several times earlier, it is not easy to gain insight into the bonding mechanisms by considering the partial occupation numbers and partial pressures in our model, since the actual values depend on how the ratios between atomic-sphere radii are chosen. Nevertheless, since we choose the *same* ratios in all compounds, it may be hoped that some conclusions can be drawn by comparing data for two compounds in the same structure. In Table VI we list the occupation numbers and excess charges for the constituents in Li_3Sb and Cs_3Sb calculated at their respective equilibrium volumes. With the reservations taken above, we do note remarkable differences between the charge distributions shown in Table VI. Antimony appears in Cs_3Sb to be strongly negatively charged, whereas it is *positive* in Li_3Sb. The numbers suggest that the cesium atom at position "D" ($Cs_{(2)}$) in Cs_3Sb is a positive ion. The Li atom at the equivalent position in Li_3Sb is almost neutral. This trend is qualitatively also what we would expect from the differences in size of the alkali-metal atoms in the two compounds. In general, the values of ΔQ, due to the model dependence (atomic-sphere—radius ratio), cannot be interpreted as meaningful physical quantities, "charge transfers," giving ionicities of the constituents. Only in cases where charge is transferred to the inner part of a sphere does such an interpretation make sense. CsAu represented[54,55] such a case, and guided by the success of the analysis of the bonding nature of this compound, we have also—for Cs_3Sb and Li_3Sb—examined the radial dependences of charge redistributions upon alloy formation.

The charge redistributions, Figs. 38 and 39, were obtained by subtracting, from the radial electron density around a constituent atom, say Sb, in the compound, the density calculated self-consistently for a pure solid (Sb in all positions A, B, C, and D) in the *same* structure and at the *same* volume (same S) as in the alloy. The distributions obtained for Cs_3Sb and Li_3Sb (Figs. 38 and 39) suggest that the bonding is quite different in the two cases, and support the idea that $Li_{(2)}$ and $SbLi_{(1)}$ is essentially neutral, and that a strong bonding occurs between Sb and its two neighboring Li atoms ($Li_{(1)}$). Thus, Li_3Sb resembles very much a molecular crystal with (neutral) $SbLi_2$ molecules and Li atoms.

The cesium compound, on the other hand, appears to be dominated by ionic bonding. Once it is assumed that the Cs on site "D" ($Cs_{(2)}$) represents a positive ion, then it is tempting to assume further that there is a strong bonding between the Sb and the two other Cs atoms [$Cs_{(1)}$, i.e., they form an ion $(SbCs_2)^-$]. The bonding between Sb and Cs appears (Fig. 38) to be ionic, Sb forming a negative ion. If this picture is correct, then the bonding of the $(Cs_2Sb)^-Cs^+$ ionic crystal should resemble that of CsI since $SbCs_2$ is isoelectronic with I. We have checked this hypothesis by calculating the change in radial Cs electron density due to compound formation in CsI ($B32$ as well as $B2$ structure). For CsI we chose the same atomic volumes (same S) as for Cs_3Sb. This turns out not to be far from the equilibrium value for CsI, and the radial change in the Cs charge, as shown in Fig. 40, as a function of r follows *very closely* that of Cs (type $Cs_{(2)}$, positive "D") in $SbCs_3$. Thus the effect on compound formation in CsI on the electronic distribution around Cs is the same as found in Cs_3Sb, and our picture of the ionicity in this compound is supported.

VII. CONCLUSION

The calculations discussed in the present work demonstrate that the local-density approximation in conjunction with self-consistent LMTO band-structure calculations is sufficiently accurate to predict stable crystal structures for elements and compounds. As pointed out in the main text, this observation is not new. We have further used the calculations of total energies and pressures to predict structural phase transitions not yet observed. In this context we mention that after the theoretical prediction of the phase instability of CsAu—occurring, according to the present work, around 40 kbar—*experimental* indications of a structural phase transition have been found[87] in pressure-dependent Mössbauer studies on this compound. This is being studied in more detail at the present.

The examination of the electronic properties of the Zintl phases of the I-II and I-III intermetallic compounds show that the bonding characteristics of those compounds which crystallize in the NaTl ($B32$) structure are reminiscent of those in Si, i.e., the formation of more or less complete sp^3 hybrids. This lends some support to the original[21] chemical point of view. It also follows that this bonding picture, among the existing Li—group-III-atom compounds, is most obvious in the case of LiAl, whereas the covalent bonding between the Tl atoms in LiTl (in a hypothetical $B32$ structure) is the weakest. These conclusions have been obtained in two ways: (i) by calculating electron densities, and (ii) from the "frozen-potential" approach. Most directly, they follow from calculations of the nonspherical charge distributions. The covalency of the bonding is most pronounced for those compounds which have band structures (in $B32$) with the smallest band overlap, i.e., with the least metallic character. LiB is in this sense an extreme case. It is the only semiconductor in this family, and has many similarities with diamond

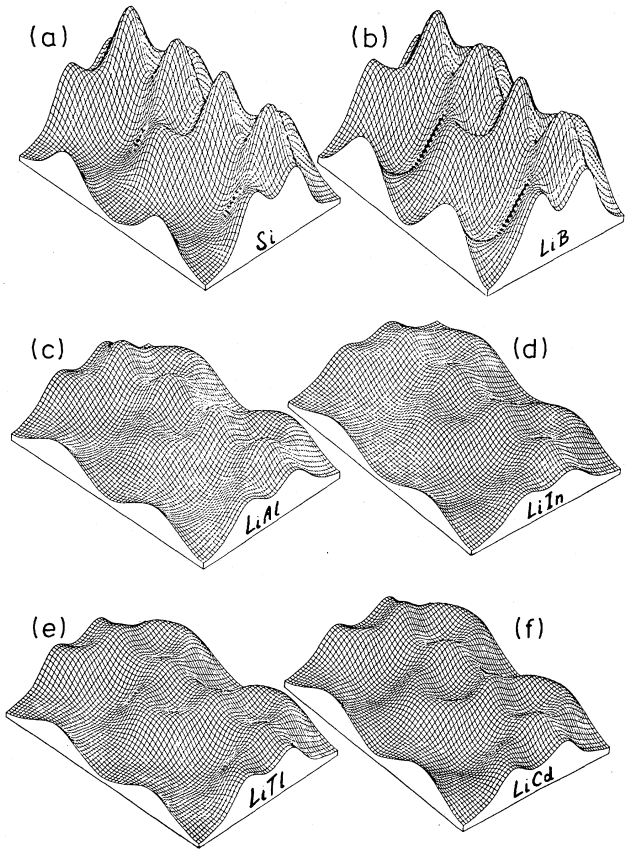

FIG. 41. (a) The pseudo-MTO density in the (110) plane of Si. The "mountain peaks" represent the bond charge between the Si atoms. (b) Pseudo-MTO density for LiB in the $B32$ structure. The density maxima—the bond-charge maxima between the B sites—have essentially the same values as in the case of Si [Fig. 40(a)]. (c)—(f) Same as (b), but for LiAl, LiIn, LiTl, and LiCd, respectively.

(the predicted bulk modulus, ~ 1.7 Mbar, is large, but smaller than that of diamond). The trends in the bonding character are summarily illustrated by Figs. 41(a)—41(f). These figures show the pseudo-MTO densities in the (110) planes of Si, LiB, LiAl, LiIn, LiTl, and LiCd, all calculated for $B32$ (LiTl in reality has the CsCl structure). This series of figures clearly shows the transition from strongly covalent bonding to an almost perfect metallic density distribution. The trends of the calculated structural energy differences, as well as those found in the calculated pressures for transitions from the $B32$ to the $B2$ structure, follow this bonding picture.

The frozen-potential calculations have made possible a separation of structural energy difference into essentially a band-structure term and an electrostatic term. The established approximate connection between our "band-structure term" and the stabilization energies obtained from pseudopotential perturbation theory gives support to the qualitative conclusions drawn from calculations of the latter type.

The I-II and I-III intermetallic compounds which, at ambient conditions, crystallize in the sodium-thallide structure, are predicted to undergo a phase transition to the cesium-chloride structure under pressure. In the frozen-potential approach this is found to be a consequence of the more rapid increase in magnitude of the Madelung energy in the $B2$ than in the $B32$ structure when the lattice dimensions are reduced. This is partly a simple "geometrical" effect caused by the different number of unlike nearest neighbors in the two structures, but it is further enhanced by the larger "charge transfer" in $B2$ than in $B32$ (cf., e.g., Fig. 11). This is caused by the valence electrons of the II- or III-constituent-atom valence electrons, and this tendency is larger the larger the nonalkali atom is. This explains why it is easier to provoke the phase transition in LiIn than in LiAl. The *compositional* phase transition with increasing atomic number, Z_M, of the group-III or -II atom is thus, from the analysis of the *pressure*-induced phase transition, considered a *size effect.* This is not much different from the arguments presented by McNeil *et al.*[78] We do not see any conflict between this model and the bonding description outlined above, i.e., the picture of sp^3-like bonding which becomes gradually "weaker" with increasing Z_M. During the preparation of this paper, we learned that Schmidt[88] has examined the electronic structure and calculated the $B2-B32$ structural energy difference for LiTl and NaTl. This work[88] also relates the structural stability criteria to "size effects." It has also been brought to our attention that our finding of a large Li p occupancy in the Li compounds and the importance of these states in the binding mechanism agree with the conclusion made for $Li_{12}Si_7$ and Li_8MgSi_6 by Böhm *et al.*[89] and Ramirez *et al.*[90]

The electronic structure calculations for the pnictide salts Li_3Sb and Cs_3Sb demonstrate that—although in these cases we did not calculate the *nonspherical* charge distributions—the antimony tends to form, via covalent-ionic bonding, an "ion" together with two nearest-neighbor alkali-metal atoms. Whereas Li_3Sb appears to be almost nonionic, i.e., $\sim Li(Li_2Sb)$, where the "single" Li site is almost neutral, we find that the ionicity of Cs_3Sb is much more pronounced. The compound is approximately described as $Cs^{\delta+}$ $(Cs_2Sb)^{\delta-}$, and it was found that the (radial) charge redistribution due to compound formation around the $(\frac{1}{2},\frac{1}{2},\frac{1}{2})$-positioned Cs atom is very similar to that found in CsI. An investigation, not presented here, further shows other similarities between the electronic structures and pressure dependences of the band structure for these two compounds. (Pressure-induced phase transitions and insulator-metal transitions in CsI are discussed elsewhere.[91,92]) For Cs_3Sb the electronic structure calculations further demonstrated the necessity of treating the Cs $5p$ states as band states, i.e., by not including them in a "frozen," renormalized core. This relaxation affects not only the calculated binding characteristics (cf. the calculated enthalpy of formation, Table III), but also, due to hybridization, the gap (see also Ref. 33).

ACKNOWLEDGMENTS

The present work was initiated by discussions with H. G. von Schnering, who is thanked for many helpful sug-

gestions. Further, the author has benefited from fruitful discussions with O. K. Andersen, F. Hensel, E. Hellner, R. Nesper, and W. B. Pearson. We thank P. C. Schmidt for communicating his results prior to publication. F. Sommer kindly supplied information about published and unpublished results of the experimental determination of heats of formation.

*Permanent address: Physics Laboratory I, Technical University of Denmark, DK-2800 Lyngby, Denmark.

[1]P. Hohenburg and W. Kohn, Phys. Rev. **136**, B864 (1964).
[2]W. Kohn and L. J. Sham, Phys. Rev. **140**, A1133 (1965).
[3]L. Hedin and B. I. Lundqvist, J. Phys. C **4**, 2064 (1971).
[4]U. von Barth and L. Hedin, J. Phys. C **5**, 1629 (1972).
[5]O. Gunnarsson and B. I. Lundqvist, Phys. Rev. B **13**, 4274 (1976).
[6]M. T. Yin and M. L. Cohen, Phys. Rev. Lett. **45**, 1004 (1980); Phys. Rev. B **25**, 7403 (1982); *ibid.* **26**, 5668 (1982).
[7]H. L. Skriver, Phys. Rev. Lett. **49**, 1768 (1982); Phys. Rev. B **31**, 1909 (1985).
[8]A. K. McMahan and J. A. Moriarty, Phys. Rev. B **27**, 3236 (1983).
[9]J. C. Boettger and S. B. Trickey, Phys. Rev. B **29**, 6425 (1984); **29**, 6434 (1984).
[10]O. K. Andersen, Phys. Rev. B **12**, 3060 (1975).
[11]D. R. Hamann, M. Schlüter, and C. Chiang, Phys. Rev. Lett. **43**, 1494 (1979).
[12]L. Kleinman, Phys. Rev. B **21**, 2630 (1980).
[13]G. B. Bachelet and M. Schlüter, Phys. Rev. B **25**, 2103 (1982); G. B. Bachelet, D. R. Hamann, and M. Schlüter, *ibid.* **26**, 4199 (1982).
[14]J. Callaway, X. Zon, and D. Bagayoko, Phys. Rev. B **27**, 631 (1983).
[15]C. S. Wang and B. M. Klein, Phys. Rev. B **24**, 3393 (1981).
[16]K.-M. Ho, C. L. Fu, B. N. Harmon, W. Weber, and D. R. Hamann, Phys. Rev. Lett. **49**, 673 (1982).
[17]O. H. Nielsen and R. M. Martin, Phys. Rev. Lett. **50**, 697 (1983).
[18]M. T. Yin and M. L. Cohen, Phys. Rev. B **26**, 3259 (1982).
[19]M. Cardona, K. Kunc, and R. M. Martin, Solid State Commun. **44**, 1205 (1982).
[20]N. E. Christensen, Solid State Commun. **49**, 701 (1983).
[21]E. Zintl and G. Brauer, Z. Phys. Chem. Abt. B **20**, 245 (1933).
[22]K. Kishio and J. O. Brittain, J. Phys. Chem. Solids **40**, 933 (1979).
[23]J. R. Willhite, N. Karnezos, P. Christea, and J. O. Brittain, J. Phys. Chem. Solids **37**, 1073 (1976).
[24]T. Asada, T. Jarlborg, and A. J. Freeman, Phys. Rev. B **24**, 510 (1981).
[25]T. Asada, T. Jarlborg, and A. J. Freeman, Phys. Rev. B **24**, 857 (1981).
[26]D. E. Ellis, G. A. Benesh, and E. Byrom, Phys. Rev. B **16**, 3308 (1977).
[27]A. Zunger, Phys. Rev. B **17**, 2582 (1978).
[28]W. Hückel, *Structural Chemistry of Inorganic Compounds,* translated by A. H. Long (Elsevier, Amsterdam, 1951), Vol. II, p. 83.
[29]D. M. Ceperley and B. J. Alder, Phys. Rev. Lett. **45**, 566 (1980).
[30]J. Perdew and A. Zunger, Phys. Rev. B **23**, 5048 (1981).
[31]A. H. MacDonald and S. H. Vosko, J. Phys. C **12**, 2977 (1979).
[32]N. E. Christensen, Phys. Rev. B **30**, 5753 (1984).
[33]G. B. Bachelet and N. E. Christensen, Phys. Rev. B **31**, 879 (1985). The importance of including the combined-correction term in the cases of elemental tetrahedral semiconductors has been stressed by D. Glötzel (private communication and Ref. 47).
[34]N. E. Christensen (unpublished).
[35]H. L. Skriver (private communication).
[36]D. Glötzel and O. K. Andersen (unpublished), and private communication.
[37]A more detailed discussion of "muffin-tin corrections" to total-energy differences calculated self-consistently or by "frozen-potential" approaches (see Sec. V B) will be given elsewhere [O.K. Andersen and N. E. Christensen (unpublished)]. See also Ref. 91.
[38]A. R. Mackintosh and O. K. Andersen, in *Electrons at the Fermi Surface,* edited by M. Springford (Cambridge University Press, Cambridge, 1979), Sec. 5.3.11. See also V. Heine, in *Solid State Physics,* edited by H. Ehrenreich, F. Seitz, and D. Turnbull (Academic, New York, 1980), Vol. 35, p. 1, Sec. 16b.
[39]Such work is in progress, and approximate contributions from the nonsphericity can be calculated in a rather simple scheme (Ref. 40).
[40]N. E. Christensen, Phys. Rev. B **29**, 5547 (1984).
[41]F. Laves, in *Intermetallic Compounds,* edited by J. H. Wesbrook (Wiley, New York, 1967), p. 129.
[42]A. E. Dwight, in *Intermetallic Compounds,* Ref. 41, p. 166.
[43]W. Freyland, in *Landolt-Börnstein, New Series, Group III,* edited by O. Madelung (Springer, Berlin, 1983), Vol. 17c p. 123.
[44]A. Goltzené and C. Schwab, in *Landolt-Börnstein, New Series, Group III,* Ref. 43, p. 137.
[45]W. B. Pearson, *The Crystal Chemistry and Physics of Metals and Alloys* (Wiley-Interscience, New York, 1972).
[46]T. Jarlborg and A. J. Freeman, Phys. Lett. **74A**, 349 (1979); see also J. Keller, J. Phys. C **4**, L85 (1971).
[47]D. Glötzel, B. Segall, and O. K. Andersen, Solid State Commun. **36**, 403 (1980).
[48]N. E. Christensen, Int. J. Quant. Chem. **XXV**, 233 (1984); A. Blacha, M. Cardona, N. E. Christensen, S. Ves, and H. Overhof, Solid State Commun. **43**, 183 (1982).
[49]The inclusion of "empty spheres' in the LMTO calculations appears to account to a large extend for the nonsphericity of the charge distribution. This follows from the comparison between *ab initio* pseudopotential calculations and the LMTO calculations for GaAs using the same prescriptions for exchange correlation; G. B. Bachelet and N. E. Christensen, Phys. Rev. B **31**, 879 (1985).
[50]The introduction of the empty spheres further offers a practical, although not physically well-founded, way of modifying, in the self-consistent calculations, the *s*-like conduction bands of the tetrahedral semiconductors. These empty conduction bands of the semiconductors are systematically predicted (Ref. 33) to lie too low in energy by the LDA, and the error cannot be considered as a constant shift in energy. Also, **k** dispersions are in error. Adjustment of the GaAs bands is discussed in Ref. 51.
[51]N. E. Christensen and M. Cardona, Solid State Commun. **51**, 491 (1984); N. E. Christensen, Phys. Rev. B **30**, 5753 (1984).
[52]H. W. A. M. Rompa, M. F. H. Schuurmans, and F. Williams, Phys. Rev. Lett. **52**, 675 (1984).
[53]N. E. Christensen, Phys. Rev. B (to be published).

[54]C. Koenig, N. E. Christensen, and J. Kollar, Phys. Rev. B **29**, 6481 (1984).

[55]N. E. Christensen and J. Kollar, Solid State Commun. **46**, 727 (1983).

[56]N. E. Christensen and G. B. Bachelet, in *Proceedings of the 17th International Conference on Semiconductor Physics, San Francisco, August 6—10 1984,* edited by D. Z. Chadi and W. A. Harrison (Springer, Berlin, in press).

[57]M. Hanfland and K. Syassen (unpublished), and private communication. M. Hanfland, K. Syassen, and N. E. Christensen, J. Phys. (Paris) Colloq. Suppl. 11, **45**, C8-57 (1984).

[58]Note that we do not claim that theory unambiguously predicts that the high-pressure phase of the compound is the $B32$ structure. The $B32$ structure indeed has, according to the calculations, a lower free energy for $P > P_t$, but we have not examined whether there might be other crystal structures for which the free energy is still lower. The theory thus only predicts that for $P > P_t$ the CsCl structure is not the stable one.

[59]W. B. Pearson, *A Handbook for Lattice Spacings and Structures of Metals and Alloys* (Pergamon, New York, 1967).

[60]Note—as for CsAu—the theory can only make a prediction about which structure among those *selected* for comparison is the most stable one. Thus we conclude here that at $P=0$, the CsCl structure is *not* the stable one. The *actual* zero-pressure structure may, however, be different from $B32$. At stoichiometric composition, LiAu probably crystallizes in an orthorhombic structure (β_2); see G. Kineast and J. Verma, Z. Anorg. Allgem. Chem. **310**, 143 (1961).

[61]The calculations for CsAu presented here treat the Cs $5s$ and $5p$ states as renormalized "frozen" core states. The effects on bonding due to self-consistent relaxation of these states, i.e, by treating them as band states, have been discussed in Refs. 54 and 55.

[62]Obviously, the separation of the total electronic pressure in a compound into "partial pressures" is somewhat ambiguous. The "l-pressure" values depend on how space is divided into regions related to each constituent atom, i.e., on the choice of the ratios between the atomic sphere radii. In general, the pressure of a compound has (of course, also depending on these radius-ratios) a Madelung contribution which cannot be split into "partial pressures." We have, in all the calculations presented here, chosen the radii of all constituents of an alloy to be equal. This also applies to the "empty spheres," in the cases where they (e.g., GaAs) are introduced (see also Ref. 64).

[63]Qualitatively, we can easily understand why this broad Au d band produces a large, positive pressure. The small size of the lattice constant in LiAu implies that there is a large overlap between the tails of (neglecting for a moment hybridization) "pure" gold d states and the Li sphere. Thus Au d states are transferred to Li; in other words, the actual Au states are strongly hybridized with Li states. This causes a loss of Au d states (the actual calculations show that as much as one Au d electron is lost when comparing it to the free atom). The states in the bottom of the Au d band are those which have the longest range, the largest amplitude in the outer part of the Au sphere. These *bonding* states are therefore predominantly lost by the hybridization, and as a result the remaining Au d states are mainly of antibonding character, i.e., the Au d pressure is positive. Simultaneously, this explains, when seen from the Li site, why the Li p states "generated" by the strong hybridization are bonding, i.e., they give a negative pressure.

[64]The number of electrons associated with each constituent also depends, of course, on how space is divided. The excess numbers of electrons depend on the atomic-sphere—radius ratios, and they cannot, in general, be considered as physically significant quantities and cannot be called "charge transfers." The very ionic compounds, like CsAu, may to some extent be considered as exceptions from this rule (see Refs. 54 and 55).

[65]It probably does not make much sense at this point to try to discuss whether the increase in p occupancies should be considered as an intersite or intrasite promotion, i.e., whether Li $s \rightarrow$ Li p and Tl $s \rightarrow$ Tl p or Li $s \rightarrow$ Tl p and Tl $s \rightarrow$ Li p. Such discussions become even more unrealistic when it is realized that there is no unambiguous way to divide space into a "Li region" and a "Tl region."

[66]O. Kubaschewski and E. L. Evans, in *Metallurgical Thermochemistry,* 3rd ed. (Pergamon, London, 1958).

[67]I. Barin, O. Knacke, and O. Kubaschewski, *Thermochemical Properties of Inorganic Substances* (supplement) (Springer, Berlin, 1977).

[68]F. Sommer (unpublished), and private communication.

[69]F. Sommer, B. Fischer, and B. Predel, in *Material Behavior and Physical Chemistry in Liquid Metal Systems,* edited by H. U. Borgstedt (Plenum, New York 1982).

[70]F. Sommer, D. Eschenweck, B. Predel, and W. R. Smutzler, Ber. Bunsenges. Phys. Chem. **84**, 1236 (1980).

[71]O. K. Andersen (unpublished).

[72]O. K. Andersen, H. L. Skriver, H. Nohl, B. Johansson, Pure Appl. Chem. **52**, 93 (1980).

[73]H. L. Skriver, *The LMTO Method,* Vol. 41 of *Springer Series in Solid-State Sciences* (Springer, Berlin, 1984), Chap. 7.

[74]LiB has not been observed. According to our calculations, LiB should be extremely stable in $B32$. Although the Li atom is "large" the core is still so small that we cannot see any size arguements against the existence of LiB in $B32$ in spite of the small (theoretical) equilibrium volume (Table III).

[75]O. K. Andersen and N. E. Christensen, Phys. Rev. B (to be published).

[76]Derived by O. K. Andersen (Ref. 71 and references given in Ref. 38).

[77]J. E. Inglesfield, J. Phys. C **4**, 1003 (1971).

[78]M. B. McNeil, W. B. Pearson, L. H. Bennett, and R. E. Watson, J. Phys. C **6**, 1 (1973).

[79]G. L. Krasko and A. B. Makhnovetskii, Phys. Status Solidi B **80**, 713 (1977).

[80]J. Hafner (unpublished), and private communication.

[81]J. Robertson, Phys. Rev. B **27**, 6322 (1983).

[82]G. M. De Munari, F. Giusiano, and G. Mambriani, Phys. Status Solidi **29**, 341 (1968).

[83]G. Wallis, Ann. Phys. (Leipzig) **17**, 401 (1956).

[84]W. E. Spicer, Phys. Rev. **112**, 114 (1958).

[85]A. H. Sommer, *Photoemissive Materials* (Wiley, New York, 1968).

[86]R. W. G. Wyckoff, *Crystal Structures,* 2nd ed. (Academic, New York, 1965).

[87]F. Hensel (private communication).

[88]P. C. Schmidt, Phys. Rev. B **31**, 5015 (1985).

[89]M. C. Böhm, R. Ramirez, R. Nesper, and H. G. v. Schnering, Ber. Bunsenges. Phys. Chem. (to be published).

[90]R. Ramirez, R. Nesper, H. G. v. Schnering and M. C. Böhm, J. Chem. Phys. (to be published).

[91]N. E. Christensen and S. Satpathy, Phys. Rev. Lett. (to be published).

[92]S. Satpathy, N. E. Christensen, and O. Jepsen, Phys. Rev. B (to be published).